

karyotypes, cytogenetic analysis was conducted by using Hoechst 33258 staining. The results showed that clones 886, 502, and 2054 maintained normal karyotype (42 chromosomes) in 20.0%, 12.5%, and 7.5 % of the cells, respectively (Fig. 4G).

DISCUSSION

In this study, we demonstrated the feasibility of homologous recombination in rat GS cells. Since this technique was first reported in 1985 [33, 34], it is the most reliable method for introducing site-directed mutations in the genome of the ES cell. The efficiency of homologous recombination varies widely among different cell types and depends on multiple factors, such as the length of homology or method of transfection. For example, the reported frequency of homologous recombination can be very high in ES cells (up to 10^{-1}) but was significantly low in fertilized eggs (1/500 eggs) [35–37]. These results raise the question as to whether this technique can be used in SSCs, another potential target of germline modification. We demonstrate that the efficiency of homologous recombination in rat GS cells was 4.2%, which is comparable to that in mouse GS cells (1.7%) and in ES cells. Therefore, our study demonstrates that a reasonable level of homologous recombination occurs in rat GS cells for their genetic manipulation.

As with other species, the most difficult part of GS cell derivation is removing testicular somatic cells. In mice, gelatin-coated plates are usually used to remove somatic cells for culture initiation [11]. As somatic cells attach firmly to gelatin-coated plates, germ cells can be enriched by gentle pipetting. However, a similar approach was not applicable to enrichment of rat germ cells because rat somatic cells proliferate more actively than mouse cells, which interfered with initial germ cell colony development. This problem was resolved by cell sorting or gentle pipetting in previous studies [22, 23]. In this study, we devised the novel method of exploiting serum-free medium and a low-cell-binding plate. Under these conditions, somatic cell proliferation is effectively suppressed during culture initiation. Unexpectedly, germ cells attached loosely to the plate and could be efficiently enriched by removing floating cells. Although cell sorting may be a useful approach for the enrichment of germ cells [23], it requires time-consuming aseptic cell separation and subsequent expansion of sorted cells. In contrast, the use of a low-cell-binding plate is relatively cost effective and does not harm the cells as much as cell sorting. The attachment of spermatogonia to a low-cell-binding plate is counterintuitive but probably does not involve integrins, because cells can be easily dislodged by gentle pipetting and cell recovery does not require trypsin digestion. The cells still proliferate slowly on the plate and form clusters within several days. This technique has worked well to establish rat GS cell lines from different genetic backgrounds in our laboratory.

Serum greatly influenced the growth of rat GS cells. Although mouse GS cells proliferate efficiently and maintain SSC activity in the presence of 1% serum [11], this concentration of serum was detrimental for rat GS cells and was reduced to ~0.2%. Perhaps some factors in the serum induce stem cell differentiation, whereas other unknown components are necessary to maintain proliferation. Despite the difference in serum concentration, rat GS cells depend critically on GDNF and FGF2 for continuous proliferation, as with mouse GS cells, and show similar morphology. While the doubling time of mouse GS cells was 5.7 days on the laminin-coated dish [16], that of the rat GS cells was 2.5 days in our study. Previous transplantation studies showed that rat germ cell colonies expand significantly faster than those of mouse in

the mouse seminiferous tubule [38]. The higher growth rate of rat GS cells on laminin-coated dishes is consistent with the in vivo observation and suggests that current culture conditions using laminin-coated dishes promote efficient growth.

Although rat GS cells proliferate stably on laminin-coated plates, they do not proliferate well on MEFs (doubling time, 3.9 days in normoxia). This is in contrast to mouse GS cells, which proliferate efficiently on MEFs (doubling time, 2.7 days) [11]. Unfortunately, although culturing on laminin was the most effective way to expand rat GS cells, we were not able to perform drug selection of two-dimensional colonies on laminin-coated plates. Drug selection was possible only with three-dimensional cluster-type colonies on MEFs. Selection under hypoxic conditions enhanced the efficiency of establishing G418-resistant clones. Hypoxia is reported to enhance survival and/or self-renewal of hematopoietic stem cells by stabilizing hypoxia-inducible factor 1 alpha [39, 40]. In another study, hypoxia prevented differentiation of human ES cells, possibly by modifying the growth factor expression pattern [41]. The mechanism of enhancement in genetic selection efficiency of GS cells in current study is unclear but may be caused by similar mechanisms. Although culture under hypoxic conditions achieved a doubling time of 3.3 days, rat GS cells still proliferated more slowly than mouse GS cells, and the colony morphology was less stable on MEFs. To resolve these problems, we tried cocultures with other feeder cells such as rat embryonic fibroblasts, STO, Sertoli cell line 15P1, and others, but we found that MEFs gave the best results in rat GS cell maintenance (our unpublished observation). Further studies are necessary to search for better selection conditions by employing other extracellular matrix or mechanical supports, which may produce three-dimensional cluster-type colonies without growth suppression.

Given that we detected a correlation between mouse strains and GS cell growth efficiency [11], we examined the influence of genetic backgrounds on rat GS cell derivation and drug selection. In mice, the genetic background significantly influenced the efficiency of GS cell derivation and maintenance. Although DBA/2 and ICR are efficient, establishing GS cells from C57BL/6 and 129 mice is difficult or impossible [11]. In contrast, the derivation of rat GS cells was not significantly influenced by the genetic background. GS cells were easily derived from all of the tested backgrounds, and we observed no significant differences in their growth rates or colony morphologies. Despite such similarity, the drug selection efficiency was significantly different among strains. The efficiency levels at which *Neo*-resistant clones were established in Wistar, BNSDF1, SDDonryuF1, and LewisSDF1 GS cells were low, but we were able to carry out genetic selection more efficiently using GS cells from DonryuSDF1 and WistarSDF1 rats. In mice, inbred strains are known to have more variable biological responses than F1 hybrids [42]. Our results suggest that genetic factors play more important roles in rat GS cells in their response to drug selection.

The most important observation in this study was the decreased germline potential of rat GS cells. While mouse GS cells could produce offspring after 2 yr of consecutive culturing or after genetic selection [13, 17], only some of the rat GS cell clones were able to undergo germline transmission. Although we obtained offspring from ROSAbetageo virus-infected cells, we were not able to do so from the two clones that underwent homologous recombination. A similar observation was also reported in a recent study using transposon-mediated mutagenesis [24]. In that study, the problem was resolved by taking advantage of *Dazl* knockdown transgenic rats with decreased

spermatogenic potential [43]. Transplanted SSCs were able to compete well with endogenous SSCs, and the recipient rats sired donor-derived offspring. In the current study, we used xenogenic transplantation to produce offspring, due to the instability of rat testes as recipients [44]; it was reported that a return of endogenous spermatogenesis is essential for reestablishing fertility after transplantation into rat recipients. We have not experienced significant problems with xenogenic transplantation with other donor cell types, but it is possible that germline potential was compromised in mouse testes and that two-targeted clones produce functional sperm if transplanted into *Dazl* knockdown transgenic rats.

Although it was speculated that the failure to undergo germline transmission might have been caused by the disruption of spermatogenic genes [24], disruption of *Ocln* is unlikely to have influenced germline potential. Although homozygous *Ocln* KO mice are infertile, heterozygous males are fertile, and no defects in spermatogenesis were found [45]; or rather, our results suggest that abnormal karyotype of the cultured cells is responsible for reduced fertility of the genetically selected cells. We currently do not know the factors directly involved in genetic stability, but we speculate that the low serum concentration might have caused abnormal karyotype. We recently found that mouse GS cells also exhibit reduced germline potential when they are cultured under serum- and feeder-free conditions [46]. The absence of serum not only decreased colony-forming efficiency after transplantation but also reduced the success rate of microinsemination. Although rat GS cells are similar to mouse GS cells in that they require serum, rat cells are more sensitive to serum, which is probably too low to maintain normal karyotype. Considering that a similar observation was also reported for human ES cells [47], it is possible that serum contains some unidentified factor that maintains chromosomal stability. We are currently improving the rat GS cell culture conditions by modifying the medium composition. In addition, as there are variations among GS cell lines, our results suggest that selection of robust GS cell lines would be necessary for successful germline transmission.

Although some GS cells underwent germline transmission, we also found placentomegaly in the offspring. A similarly large placenta is often associated with nuclear cloning [48]. However, the exact mechanism remains unknown. The abnormal placenta development in our study was likely caused by the in vitro long-term culture because we have not encountered a similar phenomenon when we carried out microinsemination using fresh round spermatids or spermatozoa, including those that were generated in the xenogenic seminiferous tubules [19, 20]. Although one of the offspring showed hypomethylation in the *Peg10* gene (Fig. 3D), no abnormal methylation was found in other offspring. Nevertheless, abnormal methylation in the *Peg10* gene suggests that this placental abnormality was caused by the disruption of other imprinting-related genes, and long-term culture and genetic selection of GS cells might also have induced epigenetic errors. These results suggest that rat GS cells are more vulnerable to stress during in vitro culture than mouse GS cells.

Currently, whether the problems associated with rat GS cells also apply to SSCs from other animal species is unknown. Although SSCs from different animals are being cultured [49–51], no attempts at genetic manipulation have been reported. Considering that rat SSCs can proliferate faster than mouse SSCs in vivo in mouse seminiferous tubules after xenogenic transplantation and that transgenic rats could be produced at a relatively high efficiency after short-term culture of SSCs [20, 43], one of the obstacles may be due to the suboptimal culture

conditions. Future studies must be directed to improve current SSC culture conditions by identifying factors that further facilitate SSC self-renewal.

In vitro expansion of SSCs and their transgenesis is a new approach in germline modification. The successful homologous recombination of rat GS cells provides an important step in extending this technique to rats. However, our study also revealed important problems associated with the genetic manipulation of GS cells that must be overcome to improve this technology. Despite these drawbacks, GS cells have the unique advantage of being able to contribute to the germline without chimera formation, which is a critical step in ES cell technology. Unlike ES cells, the phenotypes of GS cells are relatively stable [13–15]. Such advantages will allow a different approach. These unique features of SSCs make them an attractive alternative target for germline modification, with the final goal of genetically modifying SSCs from many animal species.

ACKNOWLEDGMENT

We thank Ms. Y. Ogata for technical assistance.

REFERENCES

1. Trounson A. Rats, cats and elephants, but still no unicorn: induced pluripotent stem cells from new species. *Cell Stem Cell* 2009; 4:3–4.
2. Aitman TJ, Crister JK, Cuppen E, Dominiczak A, Fernandez-Suarez XM, Flint J, Gauguier D, Geurts AM, Gould M, Harris PC, Holmdahl R, Hubner N, et al. Progress and prospects in rat genetics: a community view. *Nat Genet* 2008; 40:516–522.
3. Li P, Tong C, Mehrian-Shai R, Jia L, Wu N, Yan Y, Maxson RE, Schulze EN, Song H, Hsieh CL, Pera MF, Ying QL. Germline competent embryonic stem cells derived from rat blastocysts. *Cell* 2008; 135:1299–1310.
4. Buehr M, Meek S, Blair K, Yang J, Ure J, Silva J, McLay R, Hall J, Ying QL, Smith A. Capture of authentic embryonic stem cells from rat blastocysts. *Cell* 2008; 135:1287–1298.
5. Tong C, Li P, Wu NL, Yan Y, Ying QL. Production of p53 gene knockout rats by homologous recombination in embryonic stem cells. *Nature* 2010; 467:211–213.
6. Meistrich ML, van Beek MEAB. Spermatogonial stem cells. In: Desjardins CC, Ewing LL (eds.). *Cell and Molecular Biology of the Testis*. New York: Oxford University Press; 1993: 266–295.
7. Tegelenbosch RAJ, de Rooij DG. A quantitative study of spermatogonial multiplication and stem cell renewal in the C3H/101 F1 hybrid mouse. *Mutat Res* 1993; 290:193–200.
8. Brinster RL, Zimmermann JW. Spermatogenesis following male germ-cell transplantation. *Proc Natl Acad Sci U S A* 1994; 91:11298–11302.
9. Brinster RL, Avarbock MR. Germline transmission of donor haplotype following spermatogonial transplantation. *Proc Natl Acad Sci U S A* 1994; 91:11303–11307.
10. Kanatsu-Shinohara M, Shinohara T. The germ of pluripotency. *Nat Biotechnol* 2006; 24:663–664.
11. Kanatsu-Shinohara M, Ogonuki N, Inoue K, Miki H, Ogura A, Toyokuni S, Shinohara T. Long-term proliferation in culture and germline transmission of mouse male germline stem cells. *Biol Reprod* 2003; 69:612–616.
12. Meng X, Lindahl M, Hyvönen ME, Parvinen M, de Rooij DG, Hess MW, Raatikainen-Ahokas A, Sainio K, Rauvala H, Lakso M, Pichel JG, Westphal H, et al. Regulation of cell fate decision of undifferentiated spermatogonia by GDNF. *Science* 2000; 287:1489–1493.
13. Kanatsu-Shinohara M, Ogonuki N, Iwano T, Lee J, Kazuki Y, Inoue K, Miki H, Takehashi M, Toyokuni S, Shinkai Y, Oshimura M, Ishino F, et al. Genetic and epigenetic properties of mouse male germline stem cells during long-term culture. *Development* 2005; 132:4155–4163.
14. Liu X, Wu H, Loring J, Hormuzdi S, Distèche CM, Bornstein P, Jaenisch R. Trisomy eight in ES cells is a common potential problem in gene targeting and interferes with germ line transmission. *Dev Dyn* 1997; 209:85–91.
15. Longo L, Bygrave A, Grosveld FG, Pandolfi PP. The chromosome make-up of mouse embryonic stem cells is predictive of somatic and germ cell chimaerism. *Transgenic Res* 1997; 6:321–328.
16. Kanatsu-Shinohara M, Miki H, Inoue K, Ogonuki N, Toyokuni S, Ogura

- A. Shinohara T. Long-term culture of mouse male germline stem cells under serum- or feeder-free conditions. *Biol Reprod* 2005; 72:985–991.
17. Kanatsu-Shinohara M, Toyokuni S, Shinohara T. Genetic selection of mouse male germline stem cells in vitro: offspring from single stem cells. *Biol Reprod* 2005; 72:236–240.
 18. Kanatsu-Shinohara M, Ikawa M, Takehashi M, Ogonuki N, Miki H, Inoue K, Kazuki Y, Lee J, Toyokuni S, Oshimura M, Ogura A, Shinohara T. Production of knockout mice by random and targeted mutagenesis in spermatogonial stem cells. *Proc Natl Acad Sci U S A* 2006; 103:8018–8023.
 19. Shinohara T, Kato M, Takehashi M, Lee J, Chuma S, Nakatsuji N, Kanatsu-Shinohara M, Hirabayashi M. Rats produced by interspecies spermatogonial transplantation in mouse and in vitro microinsemination. *Proc Natl Acad Sci U S A* 2006; 103:13624–13628.
 20. Kanatsu-Shinohara M, Kato M, Takehashi M, Morimoto H, Takashima S, Chuma S, Nakatsuji N, Hirabayashi M, Shinohara T. Production of transgenic rats via lentiviral transduction and xenogeneic transplantation of spermatogonial stem cells. *Biol Reprod* 2008; 79:1121–1128.
 21. Hamra FK, Gatlin J, Chapman KM, Grellhesl DM, Garcia JV, Hammer RE, Garbers DL. Production of transgenic rats by lentiviral transduction of male germ-line stem cells. *Proc Natl Acad Sci U S A* 2002; 99:14931–14936.
 22. Ryu BY, Kubota H, Avarbock MR, Brinster RL. Conservation of spermatogonial stem cell self-renewal signaling between mouse and rat. *Proc Natl Acad Sci U S A* 2005; 102:14302–14307.
 23. Hamra FK, Chapman KM, Nguyen DM, Williams-Stephens AA, Hammer RE, Garbers DL. Self-renewal, expansion, and transfection of rat spermatogonial stem cells in culture. *Proc Natl Acad Sci U S A* 2005; 102:17430–17435.
 24. Izavák Z, Fröhlich J, Grabundzija I, Shirley JR, Powell HM, Chapman KM, Ivics Z, Hamra FK. Generating knockout rats by transposon mutagenesis in spermatogonial stem cells. *Nat Methods* 2010; 7:443–445.
 25. Friedrich G, Soriano P. Promoter traps in embryonic stem cells: a genetic screen to identify and mutate developmental genes in mice. *Genes Dev* 1991; 5:1513–1523.
 26. Morita S, Kojima T, Kitamura T. Plat-E: an efficient and stable system for transient packaging of retroviruses. *Gene Ther* 2000; 7:1063–1066.
 27. Kanatsu-Shinohara M, Inoue K, Miki H, Ogonuki N, Takehashi M, Morimoto T, Ogura A, Shinohara T. Clonal origin of germ cell colonies after spermatogonial transplantation in mice. *Biol Reprod* 2006; 75:68–74.
 28. Fujihara Y, Murakami M, Inoue N, Satouh Y, Kaseda K, Ikawa M, Okabe M. Sperm equatorial segment protein 1, SPESP1, is required for fully fertile sperm in mouse. *J Cell Sci* 2010; 123:1531–1536.
 29. Kanatsu-Shinohara M, Ogonuki N, Inoue K, Ogura A, Toyokuni S, Shinohara T. Restoration of fertility in infertile mice by transplantation of cryopreserved male germline stem cells. *Hum Reprod* 2003; 18:2660–2667.
 30. Chuma S, Nakatsuji N. Autonomous transition into meiosis of mouse fetal germ cells in vitro and its inhibition by gp130-mediated signaling. *Dev Biol* 2001; 229:468–479.
 31. Barrios F, Filippini D, Pellegrini M, Paronetto MP, Di Siena S, Geremia R, Rossi P, De Fellici M, Jannini EA, Dolci S. Offspring effects of retinoic acid and FGF9 on Nanos2 expression and meiotic entry of mouse germ cells. *J Cell Sci* 2010; 123:871–880.
 32. DiNapoli L, Batchvarov J, Capel B. FGF9 promotes survival of germ cells in the fetal testis. *Development* 2006; 133:1519–1527.
 33. Lin FL, Sperle KM, Sternberg NL. Recombination in mouse L cells between DNA introduced into cells and homologous chromosomal sequences. *Proc Natl Acad Sci U S A* 1985; 82:1391–1395.
 34. Smithies O, Gregg RG, Boggs SS, Koralewski MA, Kucherlapati RS. Insertion of DNA sequences into the human chromosomal beta-globin locus by homologous recombination. *Nature* 1985; 317:230–234.
 35. Wurst W, Joyner AL. Production of targeted embryonic stem cell clones. In: Joyner AL (ed.). *Gene Targeting*. New York: Oxford University Press; 1993: 33–61.
 36. te Riele H, Maandag ER, Berns A. Highly efficient gene targeting in embryonic stem cells through homologous recombination with isogenic DNA constructs. *Proc Natl Acad Sci U S A* 1992; 89:5128–5132.
 37. Brinster RL, Brown RE, Lo D, Avarbock MR, Oram F, Palmiter RD. Targeted correction of a major histocompatibility class II E alpha gene by DNA microinjected into mouse eggs. *Proc Natl Acad Sci U S A* 1989; 86:7087–7091.
 38. Orwig KE, Shinohara T, Avarbock MR, Brinster RL. Functional analysis of stem cells in the adult rat testis. *Biol Reprod* 2002; 66:944–949.
 39. Danet GH, Pan Y, Luongo JL, Bonnet DA, Simon MC. Expansion of human SCID-repopulating cells under hypoxic conditions. *J Clin Invest* 2003; 112:126–135.
 40. Takubo K, Goda N, Yamada W, Iriuchishima H, Ikeda E, Kubota Y, Shima H, Johnson RS, Hirao A, Suematsu M, Suda T. Regulation of the HIF-1 alpha level is essential for hematopoietic stem cells. *Cell Stem Cell* 2010; 7:391–402.
 41. Ezashi T, Das P, Roberts RM. Low O₂ tensions and the prevention of differentiation of hES cells. *Proc Natl Acad Sci U S A* 2005; 102:4783–4788.
 42. Biggers JD, Claringbold PJ. Why use inbred lines? *Nature* 1954; 174:596–597.
 43. Richardson TE, Chapman KM, Terenhaus Dann C, Hammer RE, Hamra FK. Sterile testis complementation with spermatogonial lines restores fertility to *Dazl*-deficient rats and maximizes donor germline transmission. *PLoS One* 2009; 4:e6308.
 44. Ryu BY, Orwig KE, Oatley JM, Lin CC, Chang LJ, Avarbock MR, Brinster RL. Efficient generation of transgenic rats through the male germline using lentiviral transduction and transplantation of spermatogonial stem cells. *J Androl* 2007; 28:353–360.
 45. Saitou M, Furuse M, Sasaki H, Schulzke JD, Fromm M, Takano H, Noda T, Tsukita S. Complex phenotype of mice lacking occludin, a component of tight junction strands. *Mol Biol Cell* 2000; 11:4131–4142.
 46. Kanatsu-Shinohara M, Inoue K, Ogonuki N, Morimoto H, Ogura A, Shinohara T. Serum- and feeder-free culture of mouse germline stem cells. *Biol Reprod* 2011; 84:97–105.
 47. Ludwig TE, Levenstein ME, Jones JM, Berggren WT, Mitchen ER, Frane JL, Crandall LJ, Daigh CA, Conard KR, Piekarczyk MS, Lianas RA, Thomson JA. Derivation of human embryonic stem cells in defined conditions. *Nat Biotechnol* 2006; 24:185–187.
 48. Wakayama T, Perry AC, Zuccotti M, Johnson KR, Yanagimachi R. Full-term development of mice from enucleated oocytes injected with cumulus cell nuclei. *Nature* 1998; 394:369–374.
 49. Aponte PM, Soda T, Teerds KJ, Mizrak SC, van de Kant HJ, de Rooij DG. Propagation of bovine spermatogonial stem cells in vitro. *Reproduction* 2008; 136:543–557.
 50. Kanatsu-Shinohara M, Muneto T, Lee J, Takenaka M, Chuma S, Nakatsuji N, Horiuchi T, Shinohara T. Long-term culture of male germline stem cells from hamster testes. *Biol Reprod* 2008; 78:611–617.
 51. Sadri-Ardekani H, Mizrak SC, van Daalen SK, Korver CM, Roepers-Gajadien HL, Koruji M, Hovingh S, de Reijke TM, de la Rosette JJ, van der Veen F, de Rooij DG, Repping S, et al. Propagation of human spermatogonial stem cells in vitro. *JAMA* 2009; 302:2127–2134.

Dynamic Changes in EPCAM Expression during Spermatogonial Stem Cell Differentiation in the Mouse Testis

Mito Kanatsu-Shinohara¹, Seiji Takashima¹, Kei Ishii¹, Takashi Shinohara^{1,2*}

¹ Department of Molecular Genetics, Graduate School of Medicine, Kyoto University, Kyoto, Japan, ² Japan Science and Technology Agency, CREST, Kyoto, Japan

Abstract

Background: Spermatogonial stem cells (SSCs) have the unique ability to undergo self-renewal division. However, these cells are morphologically indistinguishable from committed spermatogonia, which have limited mitotic activity. To establish a system for SSC purification, we analyzed the expression of SSC markers CD9 and epithelial cell adhesion molecule (EPCAM), both of which are also expressed on embryonic stem (ES) cells. We examined the correlation between their expression patterns and SSC activities.

Methodology and Principal Findings: By magnetic cell sorting, we found that EPCAM-selected mouse germ cells have limited clonogenic potential in vitro. Moreover, these cells showed stronger expression of progenitor markers than CD9-selected cells, which are significantly more enriched in SSCs. Fluorescence-activated cell sorting of CD9-selected cells indicated a significantly higher frequency of SSCs among the CD9⁺EPCAM^{low/-} population than among the CD9⁺EPCAM⁺ population. Overexpression of the active form of EPCAM in germline stem (GS) cell cultures did not significantly influence SSC activity, whereas EPCAM suppression by short hairpin RNA compromised GS cell proliferation and increased the concentration of SSCs, as revealed by germ cell transplantation.

Conclusions/Significance: These results show that SSCs are the most concentrated in CD9⁺EPCAM^{low/-} population and also suggest that EPCAM plays an important role in progenitor cell amplification in the mouse spermatogenic system. The establishment of a method to distinguish progenitor spermatogonia from SSCs will be useful for developing an improved purification strategy for SSCs from testis cells.

Citation: Kanatsu-Shinohara M, Takashima S, Ishii K, Shinohara T (2011) Dynamic Changes in EPCAM Expression during Spermatogonial Stem Cell Differentiation in the Mouse Testis. PLoS ONE 6(8): e23663. doi:10.1371/journal.pone.0023663

Editor: Renee A. Reijo Pera, Stanford University, United States of America

Received: May 5, 2011; **Accepted:** July 22, 2011; **Published:** August 15, 2011

This is an open-access article, free of all copyright, and may be freely reproduced, distributed, transmitted, modified, built upon, or otherwise used by anyone for any lawful purpose. The work is made available under the Creative Commons CC0 public domain dedication.

Funding: Financial support for this research was supported by the Genome Network Project, Japan Science and Technology Agency (CREST), Program for Promotion of Basic and Applied Researches for Innovation in Bio-orientated Industry, the Ministry of Health, Labour, and Welfare, The Cabinet Office, Government of Japan through its "Funding Program for Next Generation World-Leading Researchers," and the Ministry of Education, Culture, Sports, Science, and Technology (MEXT). The funders had no role in study design, data collection and analysis, decision to publish, or preparation of the manuscript.

Competing Interests: The authors have declared that no competing interests exist.

* E-mail: takashi@mfour.med.kyoto-u.ac.jp

Introduction

Spermatogonial stem cells (SSCs) account for a small population of testis cells [1,2], and their self-renewal activity distinguishes them from committed progenitor cells. Spermatogonia, the most undifferentiated germ cells in testes, contain both SSCs and progenitor cells. SSCs are able to reproduce themselves while producing progenitor cells, thereby maintaining a constant population size. In contrast, progenitor spermatogonia disappear after several rounds of mitotic division. Self-renewal activity is defined only through retrospective analysis of daughter cells, making it difficult or impossible to identify SSCs by morphological observation.

In 1994, a germ cell transplantation technique was developed, in which donor testis cells recolonize seminiferous tubules following microinjection into the testes of infertile recipients [3]. This provided the first functional assay for SSCs. The estimated number of SSCs was 2×10^3 to 3×10^3 per testis, which represents ~10% of the total A_{single} (A_s) spermatogonia, suggesting that only

a small population of A_s cells have SSC activity [2,4,5]. Using the functional transplantation assay, SSCs were subsequently analyzed for the expression of cell surface markers by selecting cells with monoclonal antibodies against surface antigens [6,7]. Although no SSC-specific markers have been identified, several markers for SSCs are available [8], and a combination of positive and negative selection by surface antigens has allowed the purification of SSCs to 1 in 15 to 30 purified cells [6,7]. However, the degree of enrichment achieved using individual antigens is limited and ranges from 1:625 to 1:1250 [6–8], suggesting that committed spermatogonia express similar markers.

In this study, we analyzed the expression of CD9 and epithelial cell adhesion molecule (EPCAM) on SSCs. CD9 is a member of the tetraspanin family molecules and is expressed on mouse and rat SSCs [9]. On the other hand, EPCAM is a homophilic, calcium-independent cell adhesion molecule and is uniquely expressed on the germline cells from the embryonic stages of germ cell development. Its expression in the postnatal testis continues until the spermatocyte stage [10]. Although both of

these antigens have been used to purify SSCs, EPCAM was the more useful marker for purifying rat SSCs [11]. However, while attempting to initiate SSC cultures from mouse testes, we observed that EPCAM-expressing cells had limited ability to produce spermatogonial colonies. Flow cytometric analysis revealed that EPCAM expression changed dynamically during spermatogonial differentiation. Here, the identity of EPCAM-expressing cells was determined by germ cell transplantation assay, and the function of EPCAM was analyzed by *in vitro* spermatogonial culture.

Materials and Methods

Ethics statement

We followed the Fundamental Guidelines for Proper Conduct of Animal Experiment and Related Activities in Academic Research Institutions under the jurisdiction of the Ministry of Education, Culture, Sports, Science and Technology, and all of the protocols for animal handling and treatment were reviewed and approved by the Animal Care and Use Committee of Kyoto University (Med Kyo 11079).

Animals

ICR mice (Japan SLC, Shizuoka, Japan) were used for primary testis cell culture. Transgenic mouse line C57BL/6 Tg14(act-EGFP)OsbY01 (designated as Green; a gift from Dr. M. Okabe, Osaka University, Osaka, Japan) was used for transplantation experiments using magnetic cell sorting (MACS). Transgenic mouse line B6-TgR(ROSA26)26Sor (designated as ROSA; purchased from the Jackson Laboratory, Bar Harbor, ME) was used for fluorescence-activated cell sorting (FACS) experiments to avoid interference of enhanced green fluorescent protein (EGFP) fluorescence for multiparameter sorting. ROSA mice that were backcrossed to the DBA/2 background for more than eight generations were used for derivation of germline stem (GS) cells [12]. WBB6F1-W/W^v (W) mice (Japan SLC) were used as recipients for germ cell transplantation.

Cell culture

For characterization of spermatogonia in the pup testis, testis cells were prepared from 7- to 10-day-old male mice. Single-cell suspensions were obtained by two-step enzymatic digestion using collagenase type IV (1 mg/ml) and trypsin (0.25%), as described previously [12,13]. Cells were plated at 3×10^5 cells / well of 6-well culture plates, which have been coated with laminin (20 μ g/ml; BD Biosciences, Franklin Lakes, NJ). GS cells were derived from ROSA mice, and were maintained on mitomycin C-treated mouse embryonic fibroblasts (MEFs) [12,13]. Culture medium was prepared by modifying commercial medium (StemPro[®]-34 serum-free medium (SFM); Invitrogen, Carlsbad, CA) as described previously [12,13]. Growth factors used were human fibroblast growth factor 2 (FGF2; 10 ng/ml) and rat glial cell line-derived neurotrophic factor (GDNF; 15 ng/ml; both from Peprotech, Rocky Hill, NJ).

For overexpression of the intracellular fragment of EPCAM (EpICD) [14], the cDNA fragment encoding EpICD (a gift from Dr. O. Gires, Ludwig Maximilian University of Munich, Germany) was cloned into *CSII-EF-IRES2-Venus* vector. Lentivirus particles were produced by transient transfection of 293T cells, and GS cells from ROSA mice (ROSA GS cells) were transfected, as described previously [15]. For EpICD overexpression experiments, the virus titer was determined by transfecting 293T cells, and the multiplicities of infection (MOI) was adjusted to 2.0. For short hairpin RNA (shRNA)-mediated gene knockdown (KD), the *Epcam* KD vectors TRCN0000111220, TRCN0000111221,

TRCN0000111222, TRCN0000111223, and TRCN0000111224 were purchased from Open Biosystems (Huntsville, AL). A mixture of lentivirus particles was used to transfect GS cells from ROSA mice, and 3 independent samples were examined. A lentivirus expressing shRNA against EGFP was used as a control (Open Biosystems). The lentivirus titer was determined using a Lenti-X p24 rapid titer kit (Clontech, Mountain View, CA). The MOI in the KD experiment was adjusted to 24.0.

Cell separation and flow cytometry

Testis cells were prepared from 5- to 10-week-old male mice. MACS was performed as described previously using rat anti-mouse EPCAM (G8.8; Biolegend, San Diego, CA) or rat anti-mouse CD9 (KMC8; BD Biosciences) antibodies [9,16]. Sheep anti-rat IgG Dynabeads (Invitrogen) were used for *in vitro* culture, and goat anti-rat IgG microbeads (Miltenyi Biotec, Gladbach, Germany) were used as a secondary antibody for FACS experiments. The average recovery was determined by four experiments.

For analyses of cell surface antigens, CD9- or EPCAM-selected cells were incubated with the following antibodies: rat anti-mouse CD9 (2B8; BD Biosciences), rat anti-mouse EPCAM (G8.8; Biolegend), mouse anti-mouse FUT4 (SSEA1; MC-480; eBioscience, San Diego, CA), biotin-conjugated anti-mouse ITGB1 (Ha2/5; BD Biosciences), and rat anti-mouse ITGA6 (GoH3; BD Biosciences). Secondary reagents were: allophycocyanin (APC)-conjugated anti-rat IgG, APC-conjugated streptavidin, and APC-conjugated anti-mouse IgM (all from BD Biosciences). For double immunostaining, CD9-selected cells were incubated with APC-conjugated rat anti-CD9 and phycoerythrin (PE)-conjugated anti-EPCAM antibodies. PE-Cy7-conjugated KIT antibody (eBioscience) was used to evaluate KIT expression in subfractionated cells. The cells were incubated in ice-cold phosphate-buffered saline/1% fetal bovine serum (PBS/1% FBS). EpICD-transfected ROSA GS cells were sorted according to Venus expression. Propidium iodide (1 μ g/ml; Sigma, St. Louis, MO) was added to exclude dead cells. Stained cells were analyzed by FACSCalibur or sorted by FACSARIA II (both from BD Biosciences).

Apoptosis assay

For terminal deoxynucleotidyl transferase dUTP nick end labeling (TUNEL) staining, single cell suspension was concentrated on glass slides by centrifugation with Cytospin 4 (Thermo Electron Corporation, Cheshire, UK). After fixation in 4% paraformaldehyde for 1 h, cells were then labeled using an *In situ* Cell Death Detection kit; TMR red (Roche Applied Science, Mannheim, Germany) following the manufacturer's protocol. The cells were counterstained with Hoechst 33342 (2 μ g/ml; Sigma) to determine the percentage of TUNEL-positive nuclei relative to the total number of cells. Apoptotic cells were quantified by collecting three images using Photoshop software (Adobe Systems, San Jose, CA). At least 200 cells were counted for each sample.

Germ cell transplantation

Germ cell transplantation was performed by microinjection into the seminiferous tubules via the efferent duct [17]. Approximately 75–85% of the tubules were filled in each recipient testis. At least three experiments were carried out for MACS and FACS. In experiments using GS cells, recipient mice were treated with anti-CD4 antibody (GK1.5; gift from Dr. T. Honjo, Kyoto University) to avoid rejection of allogeneic donor cells [18]. The Institutional Animal Care and Use Committee of Kyoto University approved all of the animal experiment protocols.

Analysis of the recipient testes

In experiments using ROSA mice, the recipient testes were fixed with 4% paraformaldehyde for 2 h, and LacZ staining was performed using 5-bromo-4-chloro-3-indolyl β -D-galactoside (X-Gal) (Wako Pure Chemical Industries, Osaka, Japan), as described previously [5]. In experiments using Green mice, the recipient testes were analyzed under UV light. These methods specifically identify donor cells, because host cells do not stain for LacZ and lack green fluorescence. We defined colonies as donor cell clusters longer than 0.1 mm occupying the entire circumference of the seminiferous tubule. Results were obtained from analyses of 10–12 recipient testes in at least two experiments. For histological analyses, samples were embedded in paraffin blocks and sectioned. The sections were counterstained with hematoxylin and eosin.

Analysis of gene expression

Total RNA was extracted using Trizol, and first-strand cDNA was synthesized by reverse transcription with SuperscriptTM II (both from Invitrogen) for reverse transcriptase-polymerase chain reaction (RT-PCR). For quantifying mRNA expression using real-time PCR, a StepOnePlusTM Real-Time PCR system and Power SYBR Green PCR Master Mix were used according to the manufacturer's protocol (Applied Biosystems, Warrington, UK). Transcript levels were normalized to that of *Hprt*, with expression levels in EPCAM-selected cells. The PCR conditions were 95°C for 10 min, followed by 40 cycles of 95°C for 15 s and 60°C for 1 min. Each PCR was run at least in triplicate using specific primers (Table S1).

Statistical analysis

The results were presented as means \pm SEM. Independent samples with equal variance were analyzed using the Student's *t*-test. SSC activity of subfractionated cells was analyzed by ANOVA followed by Tukey's HSD.

Results

Reduced SSC potential of EPCAM⁺ cells

Testicular somatic cells often overwhelm growth of proliferating germ cells in vitro [12]. To establish an improved strategy for SSC culture initiation, we assumed that EPCAM would be a useful selection marker because it is thought to be expressed specifically in germ cells, including SSCs [8,10]. In preliminary experiments, we used anti-EPCAM antibody to collect EPCAM-expressing germ cells from pup testes, which are relatively enriched for SSCs owing to the absence of differentiating germ cells [19]. Testis cells were prepared from 7-day-old pups, and EPCAM-expressing cells were collected by MACS. The cells were cultured on laminin-coated plates. Although CD9-selected cells contained testicular somatic cells that over-proliferated and interfered with germ cell proliferation in culture, the majority of the EPCAM-selected cells consisted of a pure population of germ cells; only a few somatic cells were found (Fig. 1A). However, proliferation of the EPCAM-selected cells was limited, and many of the cells eventually underwent apoptosis, which was identified by TUNEL staining (5.0 \pm 0.8% vs. 28.7 \pm 0.4%, respectively, for CD9- and EPCAM-selected cells; Fig. 1B). In contrast, cultures initiated with CD9-selected cells exhibited typical spermatogonial proliferation and colony growth by 7–10 days.

As these results indicated that EPCAM-selected cells have limited clonogenic potential in vitro, we characterized the EPCAM- and CD9-selected cells. EPCAM- and CD9-expressing cells were collected by MACS and stained for several cell surface markers known to be expressed on germline cells [8,20] (Fig. 1C).

Although both EPCAM- and CD9-selected cells expressed markers of SSCs, expression of KIT, which is a marker for progenitor spermatogonia [20], was stronger in EPCAM-selected cells, which suggested that they included more progenitor spermatogonia. In addition, CD9-selected cells also contained a significant proportion of cells that did not express EPCAM. Real-time PCR analysis of genes thought to be involved in SSC self-renewal and differentiation revealed reduced expression of *Nanos3*, *Bcl6b*, and *Elk5* in EPCAM-selected cells [8,21–23] (Fig. 1D). The expression levels of *Cnd1* and *Cnd2*, which influence SSC activity [24], were also downregulated. These results suggest that EPCAM-selected cells have reduced SSC activity.

To directly test this hypothesis, EPCAM- or CD9-expressing cells were collected and their SSC activities were assessed by germ cell transplantation. The average recoveries of EPCAM- and CD9-selected cells were 4.9 \pm 1.0% and 5.9 \pm 0.5% of the total testis cells, respectively. The selected cells were microinjected into the seminiferous tubules of congenitally infertile *W* mouse testes. Two months later, the recipients were killed, and the number of colonies in the testes was analyzed under UV fluorescence (Fig. 1E). EPCAM-selected cells produced significantly more colonies compared with non-selected control cells (5.7 \pm 1.0 vs. 1.9 \pm 0.4 colonies/10⁵ transplanted cells, respectively; Fig. 1F). In contrast, in two transplantation experiments, the CD9-selected cells resulted in more efficient SSC recovery, producing 29.5 \pm 2.3 colonies/10⁵ transplanted cells, which was 32.8 times the number of colonies from the control cells (0.9 \pm 0.6 colonies). These experiments suggest that the concentration of SSCs is higher among CD9-selected cells than EPCAM-selected cells.

Subfractionation of CD9-selected cells by EPCAM expression level

To investigate the difference between EPCAM- and CD9-selected cells in the transplantation experiments, we next analyzed the expression of EPCAM and CD9 in EPCAM- and CD9-selected cells of ROSA mice recovered by MACS. Flow cytometry of the double-stained spermatogonial populations was performed by gating according to cell size (forward scatter) and complexity (side scatter). As expected from the result of MACS experiments, CD9-selected cells contained cells with relatively high side scatter values, which suggested their heterogeneity (Fig. 2A). In contrast, EPCAM-selected cells were more uniform in size and complexity. Double-stained CD9-selected cells revealed the presence of at least three subpopulations (Fig. 2B). Fraction I consisted of cells exhibiting strong CD9 expression with relatively weak EPCAM expression. Fraction II, which contained significantly more cells than fraction I, comprised cells with strong EPCAM expression and medium CD9 expression. A CD9^{low/+} population of cells that lacked EPCAM constituted fraction III. Compared with the CD9-selected cells, the EPCAM-selected cells showed a distinct forward scatter/side scatter profile and consisted predominantly of fraction II cells. They also contained only EPCAM⁺ cells of fraction I cells (Fig. 2A). KIT expression was stronger in fraction II than in fraction I cells, suggesting that fraction I cells were more undifferentiated (Fig. 2C). Fraction III showed little KIT expression (Fig. 2C).

We then analyzed testis cells from three different developmental stages to examine when these subpopulations appear during testicular development. We collected testis cells from 1-, 10-, and 35-day-old mice and stained them with CD9 and EPCAM antibodies (Fig. 2D). Testis cells from 1-day-old mice contained only gonocytes, and showed predominantly CD9⁺ cells, with very few EPCAM⁺ cells. EPCAM⁺ cells were found in 10-day-old mouse testis cells, which contained spermatogonia and spermatocytes, but

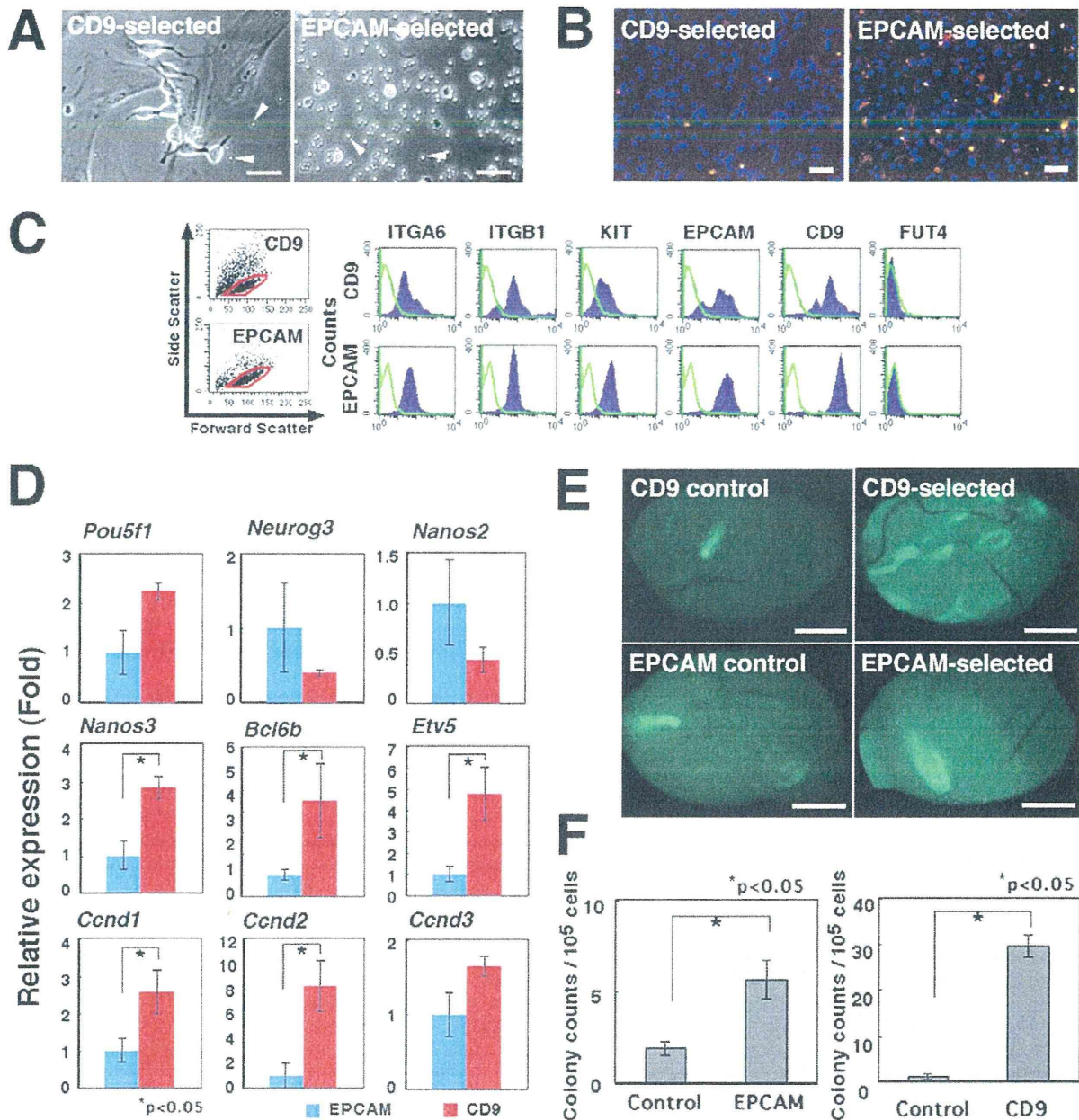


Figure 1. Characteristics of germ cells after CD9 or EPCAM selection. (A) Appearance of CD9-selected (Left) or EPCAM-selected (Right) germ cells on laminin-coated dishes, after 7 days in culture. Testis cells were collected from 10-day-old pups and used to initiate GS cell cultures after MACS. No significant colony formation is seen in EPCAM-selected cells. CD9-selected cells started to proliferate to form spermatogonia chains under the same culture condition, and spermatogonial chains are seen. Note the contaminating testicular fibroblasts in cultures of CD9-selected cells. Arrows indicate magnetic beads used for cell separation. (B) Apoptosis of CD9-selected (Left) and EPCAM-selected cells (Right), after 8 days in culture. TUNEL-positive cells are stained red. Counterstained by Hoechst 33342 (blue). (C) Flow cytometric analyses of CD9-selected (Top) or EPCAM-selected (Bottom) cells collected from adult testes. Green lines indicate control staining. Note the increased KIT staining in EPCAM-selected cells. (D) Real-time PCR analyses of spermatogonial marker genes or cyclins in EPCAM- or CD9-selected cells. CD9-selected cells show increased expression of *Nanos3*, *Bcl6b*, *Etv5*, *Ccnd1*, and *Ccnd2*. Transcript levels were normalized to *Hprt* expression, with expression levels in EPCAM-selected cells. (E) Macroscopic appearance of recipient testes transplanted with EPCAM- or CD9-selected cells. Green tubules indicate germ cell colonies developed from donor SSCs. The same numbers of cells were transplanted at the same time. (F) Quantification of colonies. Both EPCAM-selected (Left) and CD9-selected (Right) cells produced significantly more germ cell colonies than control unselected testis cells, but CD9-selected cells contained a higher concentration of SSCs. Bars = 20 μ m (A); 100 μ m (B); 1 mm (E). doi:10.1371/journal.pone.0023663.g001

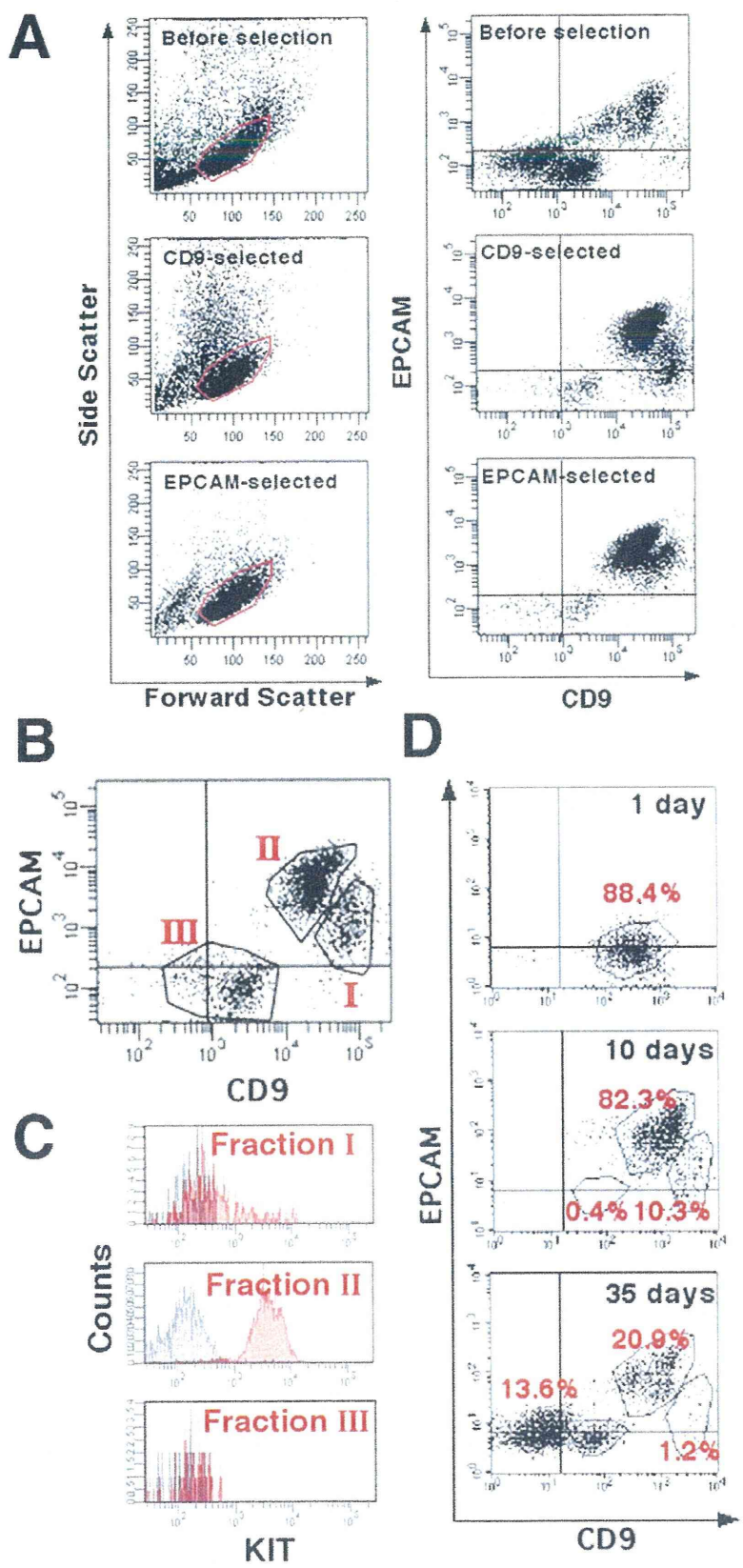


Figure 2. Flow cytometric analyses of CD9- or EPCAM-selected cells after MACS. (A) Light-scattering properties and double immunostaining of total testis cells (Top), CD9-selected cells (Middle) or EPCAM-selected cells (Bottom) stained with APC-conjugated anti-CD9 and PE-conjugated anti-EPCAM antibodies. Cells were gated according to forward scatter (size) and side scatter (cell complexity) values (Left). Gated cells were analyzed for CD9 and EPCAM (Right). Note the simpler light-scattering properties of EPCAM-selected cells. (B) Three subpopulations of CD9-selected cells. Fraction I shows high CD9 and low or no EPCAM immunostaining; fraction II shows low CD9 and high EPCAM immunostaining; and fraction III is low or no CD9 and no EPCAM immunostaining. (C) The three CD9-selected cell subpopulations, immunostained with APC-conjugated anti-CD9, PE-conjugated anti-EPCAM, and PE-Cy7-conjugated anti-KIT antibodies. KIT is strongly expressed in fraction II. Areas shaded in black indicate control staining. (D) Changes in immunostaining of total testis cells during postnatal testicular development. Total testis cells were stained with APC-conjugated anti-CD9 and PE-conjugated anti-EPCAM antibodies. Stronger CD9 and EPCAM immunostaining is seen in 10-day-old mouse testis cells compared with 1-day-old mouse testis cells. Only testes from 35-day-old mice show all three fractions. doi:10.1371/journal.pone.0023663.g002

not spermatids. Testis cells at this stage could be separated into two subpopulations, fraction I (CD9⁺EPCAM^{low/+}) and fraction II (CD9^{low}EPCAM⁺), with fraction I being significantly smaller. Testis cells from 35-day-old mice contained all stages of spermatogenic cells, and revealed three subpopulations; the relative proportion of cells in fraction I was smaller than that in 10-day-old mouse testis cells, possibly reflecting increased production of differentiating meiotic or haploid cells. These results suggest an enrichment of fraction I (CD9⁺EPCAM^{low/+}) in spermatogonia.

To determine which CD9-selected cell fraction was enriched for SSCs, cells from each of the three fractions were transplanted into the seminiferous tubules of recipient mice. Non-selected total testis cells were used as a control. Fraction I cells exhibited the highest SSC activity in recipient testes, producing 86.6 ± 24.4 colonies/ 10^5 transplanted cells (Fig. 3A and B). The concentration of SSCs in this fraction was ~ 48.7 -fold that in control cells, which produced 1.8 ± 0.5 colonies/ 10^5 transplanted cells. Consistent with this result, microscopic analysis of the sorted cells showed that fraction I consisted of cells with a relatively uniform appearance and

occasional pseudopod formation (Fig. 3A, inset). Histological sections confirmed the normal appearance of the transplanted cells (Fig. 3C). Although fraction II also contained some SSCs (1.1 ± 0.6 colonies/ 10^5 cells transplanted), no significant enrichment was observed compared with non-selected control testis cells. Fraction III cells had no SSC activity.

Analysis of EPCAM function

To investigate the function of EPCAM, we used the GS cell culture system, in which SSCs increase their numbers exponentially *in vitro* in the presence of GDNF and FGF2 [12]. GS cells were previously shown to express EPCAM, and 1–2% of GS cells had SSC activity [12,25]. Flow cytometric analyses showed that the EPCAM expression level in GS cells was upregulated by supplementation with GDNF, whereas FGF2 showed no apparent effect (Fig. 4A).

Considering the expression of EPCAM on embryonic stem (ES) cells and rat SSCs, we examined whether stimulation of EPCAM increases SSC activity. GS cells from ROSA mice were infected

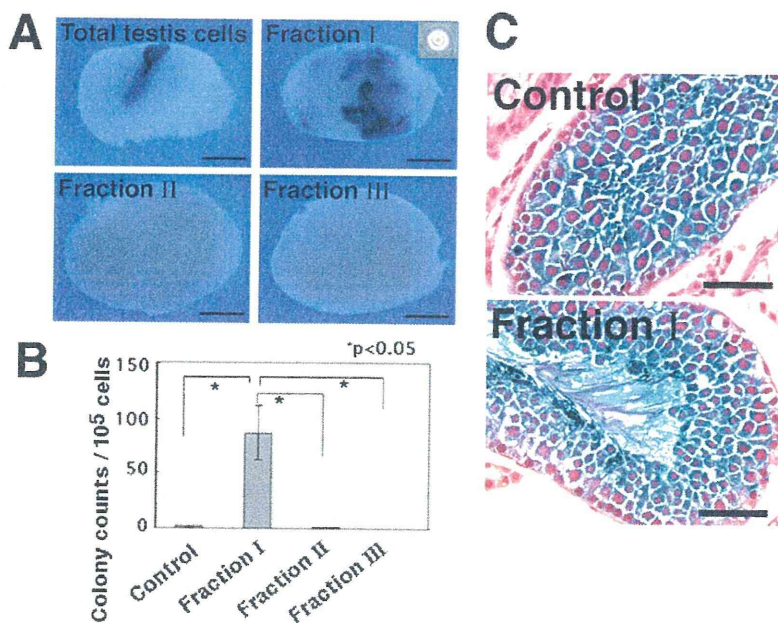


Figure 3. Functional analyses of SSC activity by germ cell transplantation of each CD9-selected cell fraction. (A) Macroscopic appearance of recipient testes. Approximately 4.9×10^3 , 2.3×10^4 , 3.5×10^2 , and 1.6×10^5 cells were transplanted for fractions I, II, III, and control cells, respectively. Recipient testes were stained with X-Gal 2 months after transplantation. Blue tubules indicate germ cell colonies developed from donor SSCs. Cells in fraction I have a uniform appearance (insert). (B) Quantification of colonies. The number of cells that could be recovered in each experiment varied, and thus the colony number was normalized to reflect donor cells at a concentration of 10^5 cells injected/testis. Cells in fraction I are significantly enriched for SSCs. (C) Histological sections of recipient testes. Note the normal appearance of spermatogenesis of donor-derived cells in recipients of control cells (Top) and fraction I cells (Bottom). Stain: X-Gal (A); X-Gal, Hematoxylin and eosin (C). Bars = 1 mm (A), 50 μ m (C). doi:10.1371/journal.pone.0023663.g003

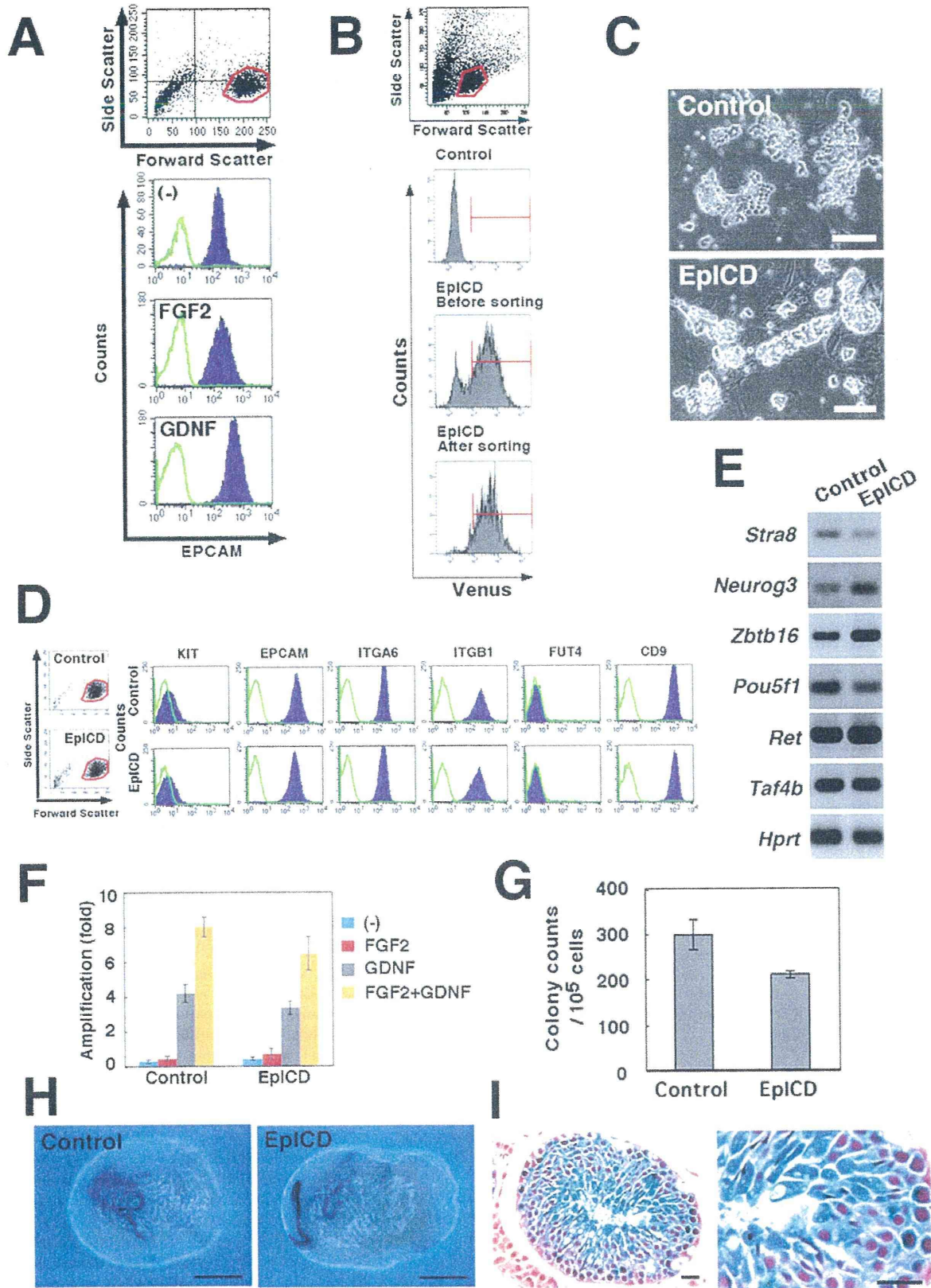


Figure 4. Overexpression of EplCD in ROSA GS cells. (A) Upregulation of EPCAM by GDNF stimulation. ROSA GS cells were cultured on laminin with 1% FBS and without cytokines for 3 days and then stimulated with the indicated cytokines. The cells were recovered 3 days after cytokine stimulation, and stained with anti-EPCAM antibody. (B) Sorting of EplCD-transfected GS cells. GS cells (3×10^5) on MEFs in 6-well plates were infected, expanded *in vitro*, and sorted. (C) Morphology of the sorted cells. (D, E) Flow cytometric (D) and RT-PCR (E) analyses of EplCD-transfected ROSA GS cells. No significant changes are seen. Green lines indicate controls. (F) Effects of cytokines on proliferation of EplCD-transfected ROSA GS cells. GS cells (3×10^5) on MEFs were cultured with the indicated cytokines and recovered by trypsinization 6 days after initiation of culture. No significant differences are seen between the control and EplCD-transfected cells. (G) Quantification of colonies. No significant differences are seen between the control and EplCD-transfected cells. (H) Macroscopic appearance of recipient testes. Recipient testes were stained with X-Gal 2 months after transplantation. Blue tubules indicate germ cell colonies developed from donor SSCs. (I) Histological sections of recipient testes. Cells show apparently normal spermatogenesis. Stain: X-Gal (H); X-Gal, Hematoxylin and eosin (I). Bars = 100 μ m (C), 1 mm (H), 20 μ m (I). doi:10.1371/journal.pone.0023663.g004

with a lentivirus expressing the intracellular domain of EPCAM (EplCD) as well as Venus protein under the control of the *EF-1* promoter. Normally in cells, EplCD is normally cleaved after EPCAM activation, and thus the EplCD protein can transmit the signal to the nucleus. Venus-expressing cells were purified and cultured *in vitro* for expansion (Fig. 4B and C). However, the transfected cells did not undergo a significant change in cell or colony morphology (Fig. 4C). In addition, flow cytometric analyses showed no change in the expression level of EPCAM or any other spermatogonial marker examined (Fig. 4D). There were no significant changes in gene expression patterns as determined by RT-PCR or in responses to exogenous cytokines (Fig. 4E and F) [8,26].

To look at the effect of EPCAM stimulation on SSC self-renewal, we transplanted EplCD-expressing GS cells into seminiferous tubules in two experiments. LacZ staining of the recipient testes showed that the numbers of colonies generated from EplCD-GS and control GS cells were 210.4 ± 8.4 and $298.1 \pm 34.1/10^5$ transplanted cells, respectively. The value for EplCD-GS cells was not significantly different from control value (Fig. 4G and H). Histological analysis of the recipient testes showed normal spermatogenesis (Fig. 4I). Thus, overexpression of EplCD did not appear to change SSC activity.

In the second set of experiments, we used shRNA to inhibit EPCAM expression. Transfection of ROSA GS cells with *Epcam* KD lentivirus vector significantly suppressed EPCAM expression within 2 days (Fig. 5A and B). EPCAM downregulation suppressed the proliferation/survival of GS cells (Fig. 5C). Only $30.4 \pm 7.6\%$ of the input cells were recovered after *Epcam* KD treatment, whereas $73.8 \pm 8.8\%$ of the input cells could be recovered after control shRNA treatment. These results indicate that EPCAM plays a role in the proliferation or survival of GS cells.

We next evaluated the SSC activity by transplanting the *Epcam* KD-transfected cells into the seminiferous tubules. Two days after infection, the cultured cells were transplanted into the testes of W mice. In two separate experiments, *Epcam* KD cells and control GS cells generated 1.6 ± 0.5 and 0.1 ± 0.1 colonies/ 10^5 transplanted cells, respectively; the difference was statistically significant (Fig. 5D and E). Thus, the *Epcam* KD treatment increased the concentration of SSCs in GS cell cultures.

Discussion

Although EPCAM has been considered as a homophilic cell adhesion molecule, a series of recent studies has shown that EPCAM, upon cleavage into small fragments, transmits proliferation signals [14,27,28]. The short intracellular domain EplCD binds to a scaffolding protein, four-and-a-half LIM domains protein 2, and is translocated into the nucleus, where it becomes part of a large nuclear complex containing CTNBN1 and LEF1, two components of the Wnt pathway. This causes upregulation of MYC and cyclins, thereby facilitating proliferation. Consistent with this, *Epcam* KD compromised proliferation of embryonic stem

(ES) cells [29]. EPCAM is also closely related to the maintenance of the undifferentiated state; EPCAM was downregulated by leukemia inhibitory factor (LIF) withdrawal, and KD treatment led to extensive differentiation [29]. As exogenously expressed EPCAM could only partially compensate for the requirement of ES cells for LIF, EPCAM is considered to be essential, but not sufficient for maintenance of the ES cell phenotype. Similar observations have also been reported for human ES cells [30,31]. However, little progress has been made on the analyses of EPCAM expression and its function in the germline.

In the present study, EPCAM expression changed dynamically during SSC differentiation. We originally hypothesized that given its strong expression on GS cells, EPCAM would be a useful antigen for selection of a pure spermatogonial population from the testis in order to initiate GS cell culture without contamination by testicular somatic cells. However, EPCAM-selected cells had limited clonogenic activity *in vitro*, and showed strong KIT expression, suggesting that they were more enriched for progenitor spermatogonia compared with CD9-selected cells. Double immunostaining and transplantation of fractionated CD9-selected cells revealed that CD9⁺EPCAM^{low/-} cells showed little KIT expression, and had significantly increased SSC activity. These results support the suggestion that EPCAM is gradually upregulated in SSCs as they differentiate into progenitor spermatogonia *in vivo*.

EPCAM upregulation during SSC differentiation was unexpected, because EPCAM has been considered a useful marker for SSCs, including those in rat and humans [11,32], and is strongly expressed on mouse GS cells. In fact, EPCAM was reported to be the best marker for rat SSCs [11]. Another study in rats also demonstrated clonogenic activity of EPCAM-expressing gonocytes [33]. Although these previous results strongly suggested that EPCAM expression in SSCs is conserved across different species, our results in mouse cells showed that EPCAM is regulated in a more sophisticated manner, being most strongly expressed in progenitor spermatogonia. The mechanism of SSC commitment has been a major topic of recent SSC research, but the lack of appropriate cell surface markers has prevented detailed analyses. EPCAM appears to be a useful cell surface marker for fractionating the spermatogonial compartment in studies of SSC self-renewal and differentiation. Our results also underscore the importance of functional transplantation studies based on the quantitative assessment of cell surface marker expression levels. It will be interesting to learn whether similar EPCAM expression patterns are conserved during spermatogenesis in other animal species.

The regulation and function of EPCAM were analyzed using GS cells, a pure proliferating spermatogonial cell population. EPCAM was upregulated by GDNF, suggesting that strong EPCAM expression in GS cell cultures is attributable in part to continuous exposure to GDNF, which is necessary for the propagation of SSCs *in vitro*. In contrast, FGF2 showed no apparent effect on EPCAM expression, although it is also an indispensable cytokine for GS cell culture. In ES cells, EPCAM

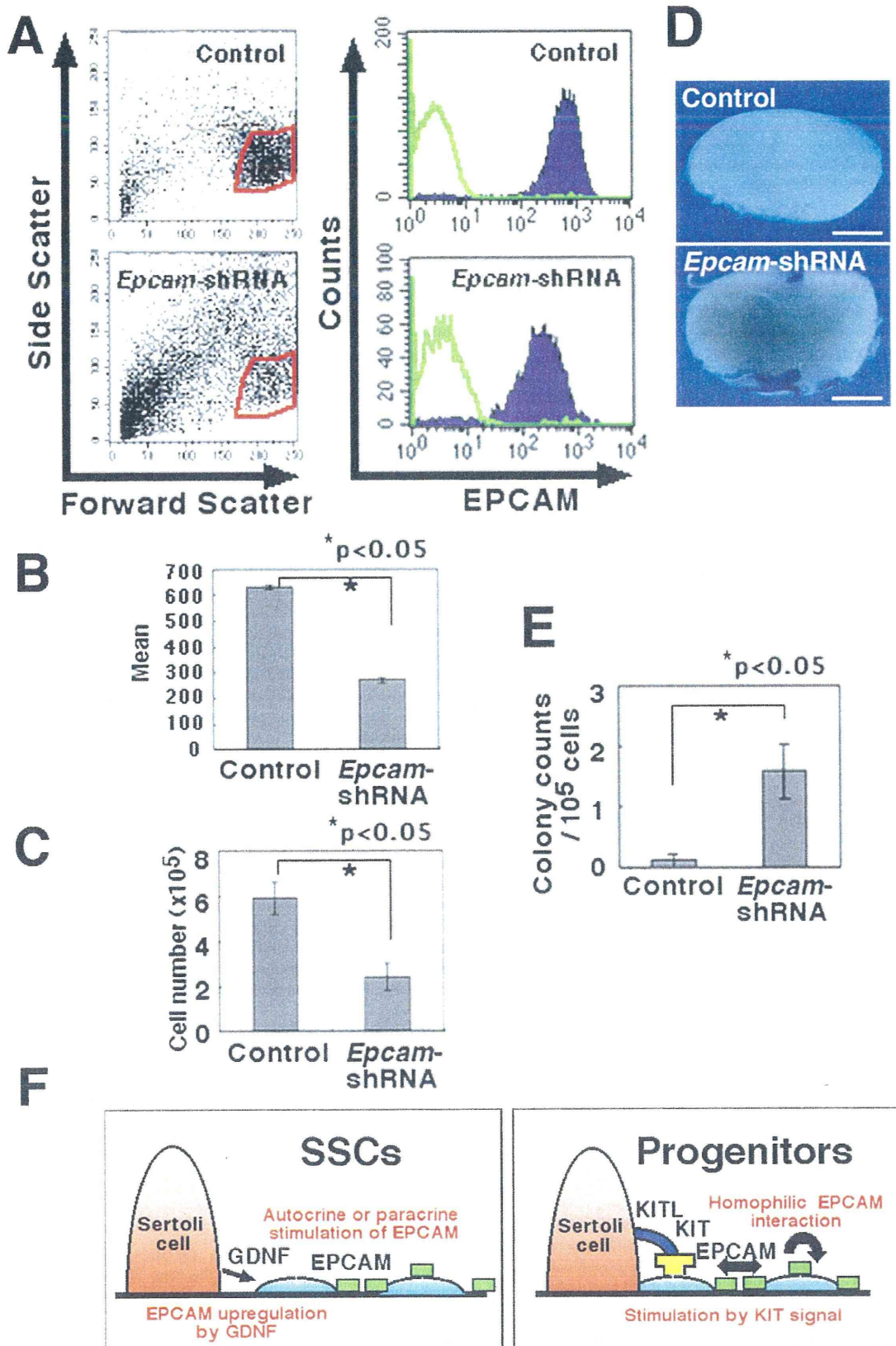


Figure 5. *Epcam* KD in ROSA GS cells by shRNA. (A) Flow cytometric profile of ROSA GS cells 2 days after transduction with *Epcam* KD vector. Green lines indicate controls. (B) Expression of EPCAM represented by the mean fluorescence intensity. Data are expressed as mean fluorescence intensity minus background autofluorescence of cells stained with the control secondary antibody. (C) Reduced recovery of ROSA GS cells after transduction with shRNA against *Epcam*. GS cells (8×10^5) on MEFs were infected with the lentivirus and recovered 2 days later. Results of three experiments are shown. (D) Macroscopic appearance of the recipient testes transplanted with *Epcam* KD GS cells. The same number of cells was transplanted at the same time. Blue tubules indicate germ cell colonies developed from donor SSCs. (E) Assessment of SSC activity by germ cell transplantation. ROSA GS cells were transplanted into the seminiferous tubules of W mice 3 days after transduction with shRNA against *Epcam*. (F) A model for EPCAM function during SSC differentiation. GDNF upregulates EPCAM expression on SSCs/progenitors. Proliferation/survival of progenitors may be stimulated by EPCAM expression on neighboring cells as well as by KITL on Sertoli cells. Stain: X-Gal (D). Bar = 1 mm (D). doi:10.1371/journal.pone.0023663.g005

expression is upregulated by LIF. Thus, our results indicate that the regulation of EPCAM expression differs between ES cells and germline cells. In GS cell culture, LIF is useful for initiating cultures from gonocytes, but is dispensable for establishment of GS cells from spermatogonia. We also have not been able to observe a positive effect of LIF on GS cell maintenance [34]. It may be that EPCAM expression changes in accordance with the cytokine milieu of the testicular microenvironment.

Although we did not find a significant effect of EpICD overexpression, the downregulation of EpICD by *Epcam* KD treatment significantly suppressed the GS cell recovery. This suggested that EPCAM is involved in proliferation or survival of spermatogonia. Interestingly, transplantation of *Epcam* KD cells resulted in a relative enrichment of SSCs. Given the in vivo expression pattern, these results suggest that EPCAM plays an important functional role in progenitor cell compartment. At present, very little is known about how progenitor spermatogonia increase their numbers in vivo. KIT is one factor involved in spermatogonial proliferation/survival [20]. Although its inhibition by neutralizing antibody kills a large number of proliferating spermatogonia [20], the inhibition of KIT signaling did not interfere with GS cell proliferation [35]. Similarly, the addition of KITL (Steel factor) did not enhance GS cell proliferation. Therefore, KIT does not appear to be vital in GS cell proliferation. The present results suggest that EPCAM may be a good candidate for progenitor cell proliferation. Cell-to-cell contact has been identified as an initial trigger for EPCAM activation [27]; therefore, we speculate that upregulated EPCAM on the cell surface may stimulate the proliferation of neighboring spermatogonia by shedding extracellular domain of EPCAM, thereby creating a positive feedback loop on proliferation signal in an autocrine or paracrine fashion [14]. This provides an additional stimulus to KIT, the ligand of which is expressed on Sertoli cells [20]. The availability of two different stimuli in parallel may perhaps contribute to the marked expansion of spermatogonia progenitors during differentiation (Fig. 5F).

The fractionation of CD9-selected cells based on EPCAM expression significantly improved the SSC purification efficiency. Subfractionation of the CD9-selected cells resulted in more efficient selection and achieved 48.7-fold enrichment. Assuming that 10% of SSCs can colonize seminiferous tubules [5], the frequency of SSCs in the suspension was 1 in 115 cells. Hence, this method appears to be more efficient than the in vivo enrichment method using cryptorchid testes, in which 1 in 161 cells were SSCs [36]. The high SSC activity in CD9⁺EPCAM^{low/+} cell population was in agreement with stronger expression of several spermatogonia molecules implicated in SSC self-renewal, including *Nanos3*, *Bcl6b*, and *Etv5* [8,22]. However, the expression level of *Nanos2*, which is thought to be expressed in the most undifferentiated spermatogonia [21], was relatively weak in the same population, possibly be due to its low expression level or the small population size.

Previous attempts to enrich SSCs were based on cryptorchid mouse models with only undifferentiated spermatogonia. Although SSCs have now been purified to 1 in 15 to 30 cells by sorting of cells from the cryptorchid testes, the preparation of cryptorchid testes requires at least 2 months to remove differentiating germ cells [36], and the technique may not be applicable to many animal species due to differences in anatomical structures. We also cannot exclude the possibility that SSCs in cryptorchid testes have different biological characteristics from those in wild-type controls. For example, a recent study showed that KIT-expressing progenitor spermatogonia from wild-type testes can generate SSCs [37]. This was in contrast to our previous study that showed the absence of KIT on SSCs collected from cryptorchid testes [6]. In the present study, SSC activity was enriched in the CD9⁺EPCAM^{low/+} cell population, which consisted predominantly of KIT^{low/+} cells. However, this population also contained some KIT⁺ cells. Although we recently reported that both KIT⁺ and KIT⁻ cell populations in GS cell culture showed comparable levels of SSC activity [35], only KIT⁻ cells showed SSC activity after transplantation, which suggested that KIT expression on SSCs may change according to their environment. Therefore, it is important to establish methods to purify SSCs from wild-type testes, and introduction of KIT as an additional marker may not only reconcile these conflicting observations but also improve the purification efficiency.

Ideally, the identification of SSC-specific antigens will greatly advance our understanding of SSC biology, as the lack of such markers has limited our knowledge regarding the regulation of SSC self-renewal and differentiation. Although the morphological description of spermatogonia has been well established, little progress has been made in the functional analysis of this compartment. Our results suggest that EPCAM is a useful marker for characterizing the spermatogonial compartment, and our analyses suggest that it plays an important role in spermatogonial progenitor proliferation or survival. The future analysis of this molecule will not only contribute to an improved SSC purification strategy but also increase our knowledge of SSC commitment.

Supporting Information

Table S1 PCR primers. (DOC)

Acknowledgments

We thank Ms. Y. Ogata for technical assistance, and Dr. O. Gires for the generous gift of EpICD cDNA.

Author Contributions

Conceived and designed the experiments: TS MKS. Performed the experiments: TS MKS KI ST. Analyzed the data: TS MKS KI ST. Contributed reagents/materials/analysis tools: TS. Wrote the paper: TS MKS.

References

- de Rooij DG, Russell LD (2000) All you wanted to know about spermatogonia but were afraid to ask. *J Androl* 21: 776–793.
- Meistrich ML, van Beek MEAB (1993) Spermatogonial stem cells. In: Desjardins CC, Ewing LL, eds. *Cell and Molecular Biology of the Testis*. New York: Oxford University Press, pp 266–295.
- Brinster RL, Zimmermann JW (1994) Spermatogenesis following male germ-cell transplantation. *Proc Natl Acad Sci USA* 91: 11298–11302.
- Tegelenbosch RAJ, de Rooij DG (1993) A quantitative study of spermatogonial multiplication and stem cell renewal in the C3H/101 F1 hybrid mouse. *Mutation Res* 290: 193–200.
- Nagano M, Avarbock MR, Brinster RL (1999) Pattern and kinetics of mouse donor spermatogonial stem cell colonization in recipient testes. *Biol Reprod* 60: 1429–1436.
- Shinohara T, Orwig KE, Avarbock MR, Brinster RL (2000) Spermatogonial stem cell enrichment by multiparameter selection of mouse testis cells. *Proc Natl Acad Sci USA* 97: 8346–8351.
- Kubota H, Avarbock MR, Brinster RL (2003) Spermatogonial stem cells share some, but not all, phenotypic and functional characteristics with other stem cells. *Proc Natl Acad Sci USA* 100: 6487–6492.
- Oatley JM, Brinster RL (2003) Regulation of spermatogonial stem cell self-renewal in mammals. *Annu Rev Cell Dev Biol* 24: 263–286.
- Kanatsu-Shinohara M, Toyokuni S, Shinohara T (2004) CD9 is a surface marker on mouse and rat male germline stem cells. *Biol Reprod* 70: 70–75.
- Anderson R, Schaible K, Heasman J, Wylie C (1999) Expression of the homophilic adhesion molecule, Ep-CAM, in the mammalian germ line. *J Reprod Fertil* 116: 379–384.
- Ryu BM, Orwig KE, Kubota H, Avarbock MR, Brinster RL (2004) Phenotypic and functional characteristics of spermatogonial stem cells in rats. *Dev Biol* 274: 158–170.
- Kanatsu-Shinohara M, Ogonuki N, Inoue K, Miki H, Ogura A, et al. (2003) Long-term proliferation in culture and germline transmission of mouse male germline stem cells. *Biol Reprod* 69: 612–616.
- Kanatsu-Shinohara M, Shinohara T (2010) Germline modification using mouse spermatogonial stem cells. *Methods Enzymol* 2010: 477: 17–36.
- Maetzel D, Denzel S, Mack B, Camis M, Went P, et al. (2009) Nuclear signaling by tumor-associated antigen EpCAM. *Nat Cell Biol* 11: 162–171.
- Kanatsu-Shinohara M, Muneto T, Lee J, Takenaka M, Chuma S, et al. (2008) Long-term culture of male germline stem cells from hamster testes. *Biol Reprod* 78: 611–617.
- Shinohara T, Avarbock MR, Brinster RL (1999) β 1- and α 6-integrins are surface markers on mouse spermatogonial stem cells. *Proc Natl Acad Sci USA* 96: 5504–5509.
- Ogawa T, Aréchaga JM, Avarbock MR, Brinster RL (1997) Transplantation of testis germinal cells into mouse seminiferous tubules. *Int J Dev Biol* 41: 111–122.
- Kanatsu-Shinohara M, Ogonuki N, Inoue K, Ogura A, Toyokuni S, et al. (2003) Allogeneic offspring produced by male germ line stem cell transplantation into infertile mouse testis. *Biol Reprod* 68: 167–173.
- Shinohara T, Orwig KE, Avarbock MR, Brinster RL (2001) Remodeling of the postnatal mouse testis is accompanied by dramatic changes in stem cell number and niche accessibility. *Proc Natl Acad Sci USA* 98: 6186–6191.
- Yoshinaga K, Nishikawa S, Ogawa M, Hayashi S, Kunisada T, et al. (1991) Role of c-kit in mouse spermatogenesis: identification of spermatogonia as a specific site of c-kit expression and function. *Development* 113: 689–699.
- Sada A, Suzuki A, Suzuki H, Saga Y (2009) The RNA-binding protein NANOS2 is required to maintain murine spermatogonial stem cells. *Science* 325: 1394–1398.
- Lilicao F, Marmo R, Paronetto MP, Pellegrini M, Dolci S, et al. (2008) Potential role of Nanos3 in maintaining the undifferentiated spermatogonia population. *Dev Biol* 313: 725–738.
- Yoshida S, Takakura A, Ohbo K, Abe K, Wakabayashi J, et al. (2004) Neurogenin 3 delineates the earliest stages of spermatogonia in the mouse testis. *Dev Biol* 269: 447–458.
- Lee J, Kanatsu-Shinohara M, Morimoto H, Kazuki Y, Takashima S, et al. (2009) Genetic reconstruction of mouse spermatogonial stem cell self-renewal in vitro by Ras-cyclin D2 activation. *Cell Stem Cell* 5: 76–86.
- Kanatsu-Shinohara M, Miki H, Inoue K, Ogonuki N, Toyokuni S, et al. (2005) Long-term culture of mouse male germline stem cells under serum- or feeder-free conditions. *Biol Reprod* 72: 985–991.
- Anderson EL, Baltus AE, Roepers-Gajadien HL, Hassold TJ, de Rooij DG, et al. (2008) Stra8 and its inducer, retinoic acid, regulate meiotic initiation in both spermatogenesis and oogenesis in mice. *Proc Natl Acad Sci USA* 105: 14976–14980.
- Münz M, Baeuerle PA, Gires O (2009) The emerging role of EpCAM in cancer and stem cell signaling. *Cancer Res* 69: 5627–5629.
- Münz M, Kieu C, Mack B, Schmitt B, Zeidler R, et al. (2004) The carcinoma-associated antigen EpCAM upregulates c-myc and induces cell proliferation. *Oncogene* 23: 5748–5758.
- Gonzalez B, Denzel S, Mack B, Conrad M, Gires O (2009) EpCAM is involved in maintenance of the murine embryonic stem cell phenotype. *Stem Cells* 27: 1782–1791.
- Ng VY, Ang SN, Chan JX, Choo ABH (2009) Characterization of epithelial cell adhesion molecule as a surface marker on undifferentiated human embryonic stem cells. *Stem Cells* 28: 29–35.
- Lu T-Y, Lu R-M, Liao M-Y, Yu J, Chung C-H, et al. (2010) Epithelial cell adhesion molecule regulation is associated with the maintenance of the undifferentiated phenotype of human embryonic stem cells. *J Biol Chem* 285: 8719–8732.
- Wu X, Schmidt JA, Avarbock MR, Tobias JW, Carlson CA, et al. (2009) Prepubertal human spermatogonia and mouse gonocytes share conserved gene expression of germline stem cell regulatory molecules. *Proc Natl Acad Sci USA* 106: 21672–21677.
- Moore TJ, de Boer-Brouwer M, van Dissel-Emiliani FM (2002) Purified gonocytes from the neonatal rat form foci of proliferating germ cells in vitro. *Endocrinology* 143: 3171–3174.
- Kanatsu-Shinohara M, Inoue K, Ogonuki N, Miki H, Yoshida H, et al. (2007) Leukemia inhibitory factor enhances formation of germ cell colonies in neonatal mouse testis culture. *Biol Reprod* 76: 55–62.
- Morimoto H, Kanatsu-Shinohara M, Takashima S, Chuma S, Nakatsuji N, et al. (2009) Phenotypic plasticity of mouse spermatogonial stem cells. *PLoS One* 4: e7909.
- Shinohara T, Avarbock MR, Brinster RL (2000) Functional analysis of spermatogonial stem cells in Steel and cryptorchid infertile mouse models. *Dev Biol* 220: 401–411.
- Barroca V, Lassalle B, Coureuil M, Lois JP, Le Page F, et al. (2009) Mouse differentiating spermatogonia can generate germinal stem cells in vitro. *Nat Cell Biol* 11: 190–196.

Rac Mediates Mouse Spermatogonial Stem Cell Homing to Germline Niches by Regulating Transmigration through the Blood-Testis Barrier

Seiji Takashima,¹ Mito Kanatsu-Shinohara,^{1,*} Takashi Tanaka,¹ Masanori Takehashi,^{1,3} Hiroko Morimoto,¹ and Takashi Shinohara^{1,2,*}

¹Department of Molecular Genetics, Graduate School of Medicine, Kyoto University, Kyoto 606-8501, Japan

²Japan Science and Technology Agency, CREST, Kyoto 606-8501, Japan

³Present address: Laboratory of Pathophysiology and Pharmacotherapeutics, Faculty of Pharmacy, Osaka Ohtani University, Tondabayashi, Osaka 584-8540, Japan

*Correspondence: mshinoha@virus.kyoto-u.ac.jp (M.K.-S.), tshinoha@virus.kyoto-u.ac.jp (T.S.)

DOI 10.1016/j.stem.2011.08.011

SUMMARY

The homing ability of spermatogonial stem cells (SSCs) allows them to migrate into niches after being transplanted into infertile testes. Transplanted SSCs attach to Sertoli cells and transmigrate through the blood-testis barrier (BTB), formed by inter-Sertoli tight junctions, toward niches on the basement membrane. The most critical step is the passage through the BTB, which limits the homing efficiency to <10%. Here we demonstrated the involvement of Rac1 in SSC transmigration. *Rac1*-deficient SSCs did not colonize the adult testes, but they reinitiated spermatogenesis when transplanted into pup testes without a BTB. Moreover, a dominant-negative Rac1 construct not only reduced the expression of several claudin proteins, which comprise the BTB, but also increased SSC proliferation both in vitro and in vivo. Short hairpin RNA (shRNA)-mediated suppression of claudin3, which was downregulated by Rac inhibition, reduced the SSC homing efficiency. Thus, Rac1 is a critical regulator of SSC homing and proliferation.

INTRODUCTION

Spermatogenesis is a complex process that originates from the continuous division of SSCs. The mouse testis contains only $2\text{--}3 \times 10^4$ SSCs per testis, accounting for 0.02%–0.03% of the total testis germ cell suspension (de Rooij and Russell, 2000; Meistrich and van Beek, 1993). Despite their small number, these cells have a unique ability to undergo self-renewal division to reproduce themselves as well as produce committed daughter cells. Accumulating evidence indicates that SSCs are not randomly distributed in the testis, but that they reside within special microenvironments called “niches” where they can remain undifferentiated (Chiarini-Garcia et al., 2001). Self-renewal factors secreted from the niche are considered to maintain SSCs in the undifferentiated state, and this unique environ-

ment is a prerequisite for self-renewal division; failure to remain in the niche induces differentiation or apoptosis. Although the precise location and cellular composition of these niches have long remained unknown, morphological analyses suggested that niches are located along the region of the basal lamina that faces the interstitium (Chiarini-Garcia et al., 2001). This area of the tubules has a relatively rich blood supply, and a recent study suggested that the germline niche is established in accordance with vasculature pattern formation (Yoshida, 2010).

Despite their close relationship, the interaction between SSCs and niches is dynamic. This is best illustrated by germ cell transplantation experiments, in which SSCs from a donor animal recolonized the seminiferous tubules when microinjected into those of infertile animals (Brinster and Zimmermann, 1994). Following introduction into the adluminal compartment of the seminiferous tubules, SSCs attach to the Sertoli cells, and within a few days migrate to the basal compartment following passage through the blood-testis barrier (BTB) between Sertoli cells. SSCs then proliferate to form chains or networks of spermatogonia on the basement membrane at around 2–3 weeks later and begin to differentiate adluminally at around 1 month, eventually producing mature spermatozoa by 2–3 months after transplantation (Nagano et al., 1999). These experiments demonstrated that SSCs have the ability to migrate toward the niche in a manner similar to hematopoietic stem cells (HSCs).

Although the homing ability of SSCs was discovered in 1994, very little is known about the molecular mechanism. However, $\beta 1$ -integrin expression in SSCs was recently shown to play a critical role in their homing ability (Kanatsu-Shinohara et al., 2008). In these experiments, the function of adhesion molecules in SSC homing was examined in *Itgb1* and *Cdh1* conditional knockout (KO) mice. These genes are strongly expressed in spermatogonia and were used as SSC markers (Oatley and Brinster, 2008). By combining with $\alpha 6$ -integrin, $\beta 1$ -integrin comprises a laminin receptor and mediates the binding of SSCs to laminin in vitro. SSCs from *Itgb1* KO mice cannot form germ cell colonies and disappear after transplantation. Loss of $\beta 1$ -integrin expression probably prevents attachment of SSCs to the basal membrane because SSCs without $\beta 1$ -integrin neither attached to laminin in vitro nor migrated into the niche, even when transplanted into pup testes without a BTB. In contrast, SSCs without E-cadherin could home into the niche and produce normal germ

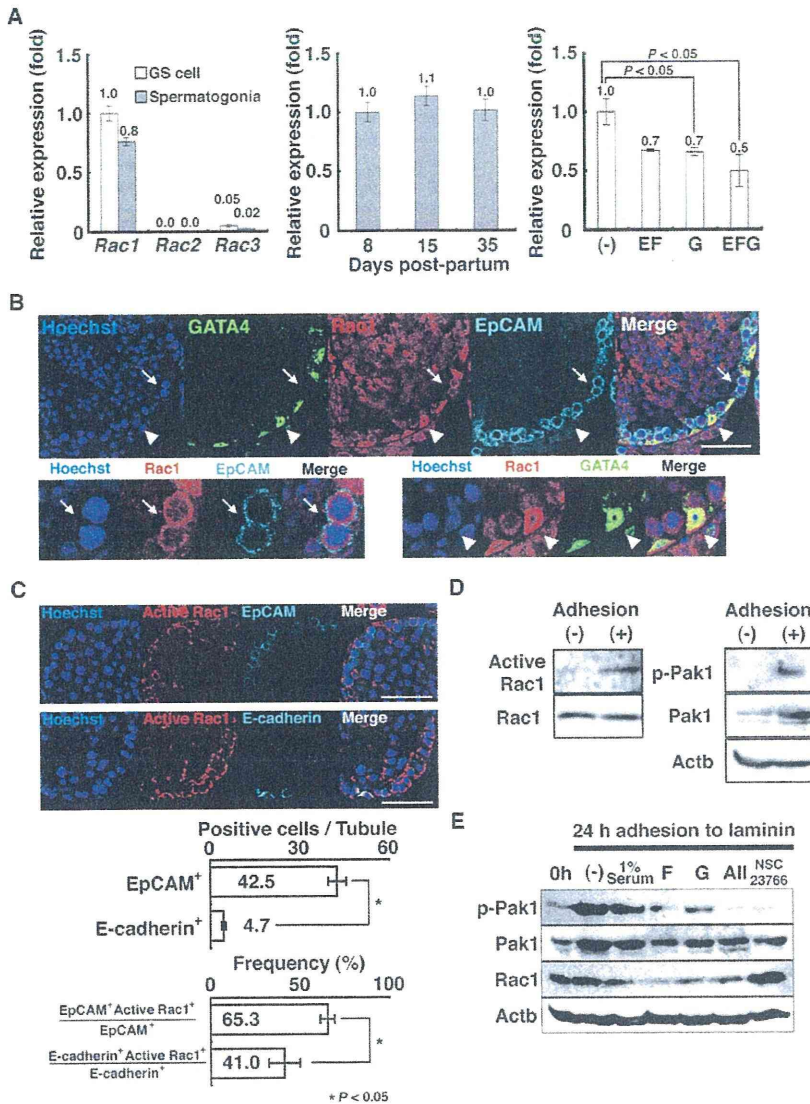


Figure 1. Expression and Activation of Rac
(A) (Left) Real-time PCR analyses of Rac expression. *Rac1* was predominantly expressed in both EpCAM⁺ spermatogonia from 8-day-old pup testes and GSCs (n = 3). (Middle) Developmental changes in *Rac1* expression in EpCAM⁺ spermatogonia. No significant changes were found (n = 3). (Right) Downregulation of *Rac1* expression in GSCs by cytokine treatment. GSCs were cultured on laminin for 3 days under the indicated culture conditions (n = 3).

(B) *Rac1* expression in 8-week-old mouse testes. *Rac1* is expressed not only in EpCAM⁺ spermatogonia (arrow) but also in GATA4⁺ Sertoli cells (arrowhead).

(C) Localization of activated Rac in spermatogonia. (Top) Immunostaining. (Middle) Calculation of EpCAM⁺ or E-cadherin⁺ cells per seminiferous tubule (n = 15). (Bottom) Quantification of cells with activated *Rac1* expression (n = 637 for EpCAM; n = 70 for E-cadherin). Activated *Rac1* was found more frequently in EpCAM⁺ spermatogonia than in E-cadherin⁺ spermatogonia. Double-positive cells on 15 tubules were counted for each cell type.

(D) Western blot analyses of *Rac1* activation. GSCs were cultured on laminin without cytokines or serum, and the samples were recovered after 24 hr. (Left) Pull-down assay of activated *Rac1*. GST-fusion proteins containing Pak1 were used to affinity-precipitate active *Rac1* from the cell lysate. (Right) The same cell lysate was used to detect phosphorylated Pak1.

(E) Effects of cytokines and *Rac* inhibitor on Pak1 phosphorylation. GSCs were cultured on laminin for 24 hr, and the indicated factors were added at the time of plating. E, EGF; F, bFGF; G, GDNF. Scale bar = 50 μ m (B and C). Error bars = SEM. See also Tables S1 and S2.

RESULTS

Expression of Rac Genes in Primary Spermatogonia and Germline Stem Cells

Spermatogonia were collected from the testes of 8-day-old pups by magnetic-activated cell sorting (MACS) using the

cell colonies and spermatozoa. These results were unexpected, because cadherin mediates the stem-cell-niche interaction in *Drosophila* gonads (Li and Xie, 2005). These experiments identified β 1-integrin as a homing receptor for SSCs.

Here, we examined the roles of *Rac1* small G protein in SSC homing. Because *Rac* is often activated downstream of the integrin receptor and mediates HSC homing (Cancelas et al., 2006), we hypothesized that *Rac* may also be involved in SSC adhesion to the basement membrane. However, our results showed that *Rac* was involved in a different step of homing, i.e., transmigration of SSCs through the BTB. We found that *Rac* regulates the expression of several claudins, critical components of the tight junction complex. Functional analyses by shRNAs showed that claudin3 downregulation is responsible for the loss of SSC activity.

SSC marker EpCAM (Oatley and Brinster, 2008). We then examined the expression of *Rac* family molecules. Within the *Rac* subfamily, real-time polymerase chain reaction (PCR) analyses showed that spermatogonia predominantly express *Rac1* (Figure 1A, left and Table S1, available online). Although *Rac3* was expressed at significantly lower levels, *Rac2* expression was not detected. Despite the increased mitotic activity of pup spermatogonia (Nagano et al., 2001), *Rac1* expression was relatively constant at three different stages (8, 15, and 35 days old; Figure 1A, middle).

To understand the effect of the environment, we examined the expression of *Rac* genes in germline stem cells (GSCs), cultured spermatogonia with enriched SSC activity (Kanatsu-Shinohara et al., 2003). GSCs proliferate in the presence of self-renewal factors, including glial-cell-line-derived neurotrophic factor

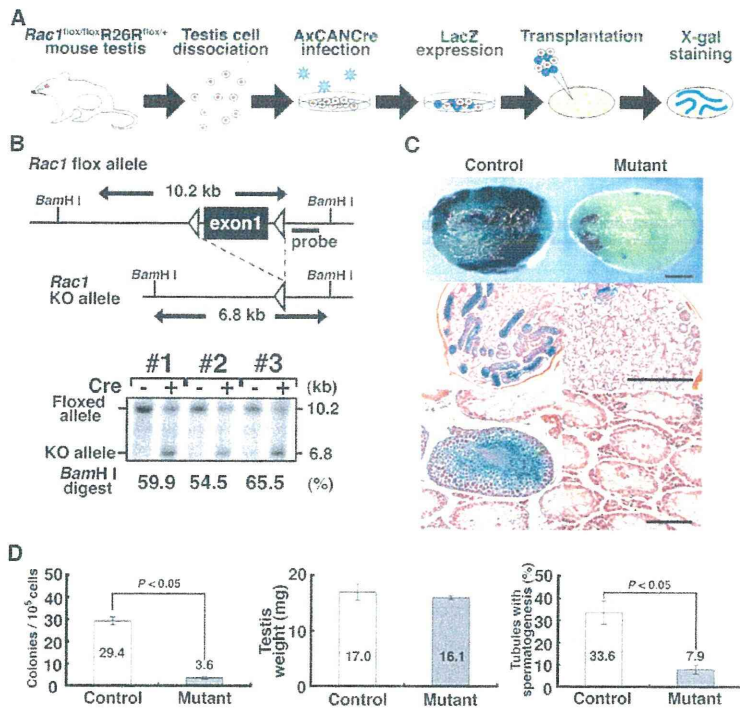


Figure 2. Reduced Colonizing Ability of *Rac1* Mutant Cells

(A) Diagram of the experimental procedure. Testes from *Rac1* conditional mutant mice were dissociated and exposed to AxCANCre in vitro overnight. Cre-mediated deletion removed the target genes, and the cells were transplanted into recipient pup or adult testes to evaluate SSC activity. The colonization levels were determined by counting tubules with spermatogenesis by histology 3 months after transplantation. The colonization levels in adult recipients were also evaluated by counting the numbers of LacZ⁺ colonies.

(B) (Top) Conditional mutant mice used in the experiment. The *Rac1* mutant strain was crossed with a ROSA26 reporter mouse strain (R26R) to visualize donor cell colonization. (Bottom) Southern blot analysis of deletion efficiency. Genomic DNA was hybridized with the indicated probe.

(C) Macroscopic (top) and histological (middle and bottom) appearances of the recipient testes. Blue tubules indicate donor cell colonization. Note the reduced colonization levels in recipients with *Rac1* mutant cells.

(D) Evaluation of donor-derived spermatogenesis. (Left) Colony count (n = 10 for control; n = 12 for mutant). (Middle) Testis weight (n = 12). (Right) Tubules with spermatogenesis (n = 15 for control; n = 14 for mutant). The numbers of tubules counted were 1,321 (control) and 1,256 (mutant).

Scale bar = 1 mm (C, top and middle); 100 μ m (C, bottom). Stain, hematoxylin and eosin (C). Error bars = SEM. See also Figure S1.

(GDNF) and epidermal growth factor (EGF)/basic fibroblast growth factor (bFGF), and produce germ cell colonies following transplantation into seminiferous tubules. Real-time PCR analyses showed that *Rac1* expression also predominated in GSCs (Figure 1A, left). Moreover, the addition of self-renewal factors inhibited *Rac1* expression. While the combination of EGF and bFGF showed a comparable effect to GDNF, the addition of all cytokines reduced the *Rac1* levels to 50% (Figure 1A, right). Because these results suggest that *Rac1* is downregulated around the niche, we performed immunostaining for *Rac1* to examine its expression in testis. *Rac1* expression was found not only in spermatogonia, but also in Sertoli cells (Figure 1B and Table S2). Also, activated *Rac1* staining was found more frequently in EpCAM⁺ cells than in E-cadherin⁻ cells (Figure 1C). Because E-cadherin is expressed in a more primitive subset of spermatogonia than those with EpCAM (Yoshida, 2010), these results suggest that *Rac* activation occurs more frequently in differentiating cells.

Using GSCs, we then performed pull-down assays to determine how *Rac1* is activated. A GST-fusion protein containing the Rac-binding domain of Pak1 was used to precipitate active *Rac1*. We examined the effects of laminin, because SSCs preferentially attach to laminin via β 1-integrin (Kanatsu-Shinohara et al., 2008). Consistent with previous studies, we found that *Rac1* was activated by adhesion to laminin-coated plates within 1 day after plating (Figure 1D, left). Due to the relatively low sensitivity of the assay, we also evaluated the *Rac* activation levels by examining Pak1 phosphorylation. Binding of *Rac* to Pak1 causes autophosphorylation of Ser residues in the amino-terminal inhibitory domain, which induces conformational changes and subsequent Pak1 activation by PDK (Knaus and Bokoch,

1998). As expected from the results of the pull-down assay, laminin binding also induced Pak1 phosphorylation (Figure 1D, right). Pak1 phosphorylation was no longer observed once the cells were detached from the laminin-coated dishes by trypsin digestion. Increases in total and phosphorylated Pak1 levels were also observed in response to laminin binding, which was probably caused by *Rac* translocation to the membrane upon binding (del Pozo et al., 2000). In contrast, addition of individual self-renewal factors reduced Pak1 phosphorylation, while serum had no significant effect (Figure 1E). A combination of all cytokines not only strongly suppressed Pak1 phosphorylation but also reduced *Rac1* protein expression, consistent with the results of real-time PCR analyses (Figure 1A, right). This Pak1 phosphorylation was inhibited by the *Rac* inhibitor NSC23766, confirming that *Rac* activation is necessary for Pak1 phosphorylation. Together, these results suggest that adhesion to laminin can activate *Rac1*, which is downregulated by self-renewal factors.

Rac1 Gene Deletion Inhibits SSC Homing after Germ Cell Transplantation

To understand the role of *Rac1* in SSC homing, we deleted the *Rac1* gene in SSCs in mice carrying a *Rac1* gene flanked by loxP sites (*Rac1* floxed mice) generated by homologous recombination (Glogauer et al., 2003) (Figure 2A). The *Rac1* mutant mouse strain was crossed with the ROSA26 reporter mouse strain (R26R) to visualize the pattern of proliferation and differentiation of mutant SSCs (Soriano, 1999). Heterozygous R26R mice were used as controls.

Testis cells were collected from 8- to 12-day-old pups by enzymatic digestion. Testes at this stage are enriched in SSCs

due to the lack of differentiated cells (Shinohara et al., 2001). Single-cell suspensions were then exposed to adenovirus expressing Cre (AxCANCre) overnight in vitro. After incubation, ~60% of the infected cells could be recovered by trypsin digestion. Cre infection did not significantly enhance apoptosis of total testis cells (Figure S1 available online). Southern blot analyses showed that $60.0\% \pm 3.2\%$ ($n = 3$) of the floxed alleles were deleted from the *Rac1* gene locus at the time of transplantation (Figure 2B). To quantify the SSC number, $\sim 1.2 \times 10^5$ testis cells were microinjected into the seminiferous tubules of WBB6F1-*W/W^v* (*W*) mice. *W* mice lack endogenous spermatogenesis and serve as recipients for donor SSCs (Brinster and Zimmermann, 1994). Three sets of experiments were carried out, and the recipient testes were recovered and stained for β -galactosidase activity with X-gal 3 months after transplantation. This period corresponds to approximately three cycles of mouse spermatogenesis, thereby providing a sufficient time window for spermatogenesis regeneration (de Rooij and Russell, 2000).

Macroscopic analyses of the recipient testes showed significant reduction of blue germ cell colonies, while transplantation of control cells resulted in extensive colonization (Figures 2C and 2D). Moreover, the mutant recipient testes showed weaker blue staining, suggesting poorer spermatogenesis recovery (Figure 2C). The average weights of the recipient testes were not significantly different (Figure 2D). We further evaluated the colonization levels of the donor cells by histological analyses. As germ cells in *W* mice cannot differentiate beyond the undifferentiated spermatogonia stage (Ohta et al., 2004), all spermatogenesis was derived from transplanted donor cells. We assessed the numbers of tubules with spermatogenesis by counting tubules with multiple layers of germ cells. In total, the mutant cells showed spermatogenesis in $7.9\% \pm 2.0\%$ ($n = 14$) tubules, while wild-type (WT) control cells showed spermatogenesis in $33.6\% \pm 5.2\%$ ($n = 15$) tubules (Figure 2D); this difference was statistically significant. These results indicated that deletion of the *Rac1* gene inhibited SSC colonization.

Analysis of Rac1 Function Using GSCs

To understand the effects of Rac1 in SSC homing, GSCs expressing a dominant-active (RacV12; DA-Rac) or a dominant-negative Rac1 (RacN17; DN-Rac) construct were produced by transfecting GSCs with enhanced green fluorescent protein (EGFP; Figure 3A). DA-Rac cells showed increased cellular protrusion, while such protrusions were rarely found in DN-Rac cells (Figure 3B). Flow cytometric analyses indicated that both DA- and DN-Rac cells had normal levels of $\alpha 6$ - and $\beta 1$ -integrins, which are considered to be involved in SSC homing (Figure 3C). We observed no significant changes in other SSC markers, such as EpCAM and CD9. The mutant cells expressed c-kit, suggesting the presence of differentiating cells. However, they did not express SSEA-1, a marker of ESCs. Reverse transcription PCR (RT-PCR) analyses also confirmed the normal spermatogonia phenotype of both DA- and DN-Rac cells (Figure 3D and Table S3). Several spermatogonia markers, including *Pou5f1*, *Zbtb16*, *Neurog3*, and *Taf4b*, were expressed in both cell types, but they did not express *Nanog*, another ESC marker. These results indicated that the changes in Rac activity did not induce apparent abnormalities in the spermatogonia phenotype.

We then evaluated the laminin binding abilities of DA- and DN-Rac cells (Figure 3E). In these experiments, GSCs were plated on laminin-coated plates, which were washed several times to remove floating cells after incubation. The cells that adhered to the plates were recovered by trypsinization. Despite the normal expression levels of $\alpha 6$ - and $\beta 1$ -integrins, DN-Rac cells showed increased adhesion to laminin. While $58.4\% \pm 4.9\%$ of the DN-Rac cells could attach to laminin-coated plates, $43.6\% \pm 4.1\%$ and $47.6\% \pm 3.8\%$ of control and DA-Rac cells, respectively, adhered after 30 min incubation ($n = 12$). However, we found no significant differences in colony morphology of DA- and DN-Rac cells on either mouse embryonic fibroblasts (MEFs) or laminin-coated dishes. The cells did not attach to the fibronectin- or collagen-type-I-coated plates. These results indicated that changes in Rac1 activity modulate laminin-binding activity.

In addition to the increased adhesion, DN-Rac cells showed more active proliferation than control and DA-Rac cells (Figure 3F). While both control and DA-Rac GSCs expanded 6.4 ± 0.3 and 6.6 ± 0.9 -fold, respectively, during 6 days, DN-Rac cells expanded 11.9 ± 0.9 -fold during the same period ($n = 6$). The effect of DN-Rac was not mimicked by NSC23766 (Figure S2), suggesting that an interaction with Rac-specific guanine nucleotide exchange factor Trio or Tiam1 is not involved in the enhanced proliferation (Gao et al., 2004). As cyclin overexpression can enhance GSC proliferation and has an impact on SSC colonization, we also examined the pattern of cyclin D expression (Lee et al., 2009). Real-time PCR analyses showed increased expression of *Ccnd1* in DA-Rac cells (Figure 3G), consistent with a previous study reporting that Rac activation increases *Ccnd1* transcription (Joyce et al., 1999). *Ccnd3* also decreased in both types of cells. However, no significant difference was seen between DN-Rac and control cells in *Ccnd2* expression, which enhances in vitro proliferation of GSCs (Lee et al., 2009). These results suggest that enhanced proliferation of DN-Rac cells was mediated by a cyclin-D2-independent mechanism.

Because Rac1 was downregulated in vitro by cytokine treatment, a serial transplantation technique was next used to examine the effects of Rac activity on SSC self-renewal under physiological conditions (Figure 4A). In these experiments, approximately 4×10^3 cells expressing the EGFP gene were microinjected into the seminiferous tubules of *W* mice (primary recipients). Two months after transplantation, the primary recipients were killed and the number of colonies in the testis was determined under UV illumination. Consistent with the decreased homing of Rac1 KO SSCs, DN-Rac cells produced significantly fewer colonies, but we found no significant difference between DA-Rac and control cells (Figures 4B and 4C). The number of cells recovered from the three types of recipients ranged from 0.5 to 1.6×10^6 cells (average of 1.1×10^6 cells). Differences between donors were not significant.

When the secondary recipients were analyzed, DN-Rac cells produced significantly fewer secondary colonies than control and DA-Rac cells (Figure 4D and Table S4). Although both control and DA-Rac cells showed increased colony numbers (total regenerated colony number – primary colony number used for transplantation) in 9/9 (100%) and 11/12 (91.7%) transplantations, only 8/12 (66.7%) transplantations showed

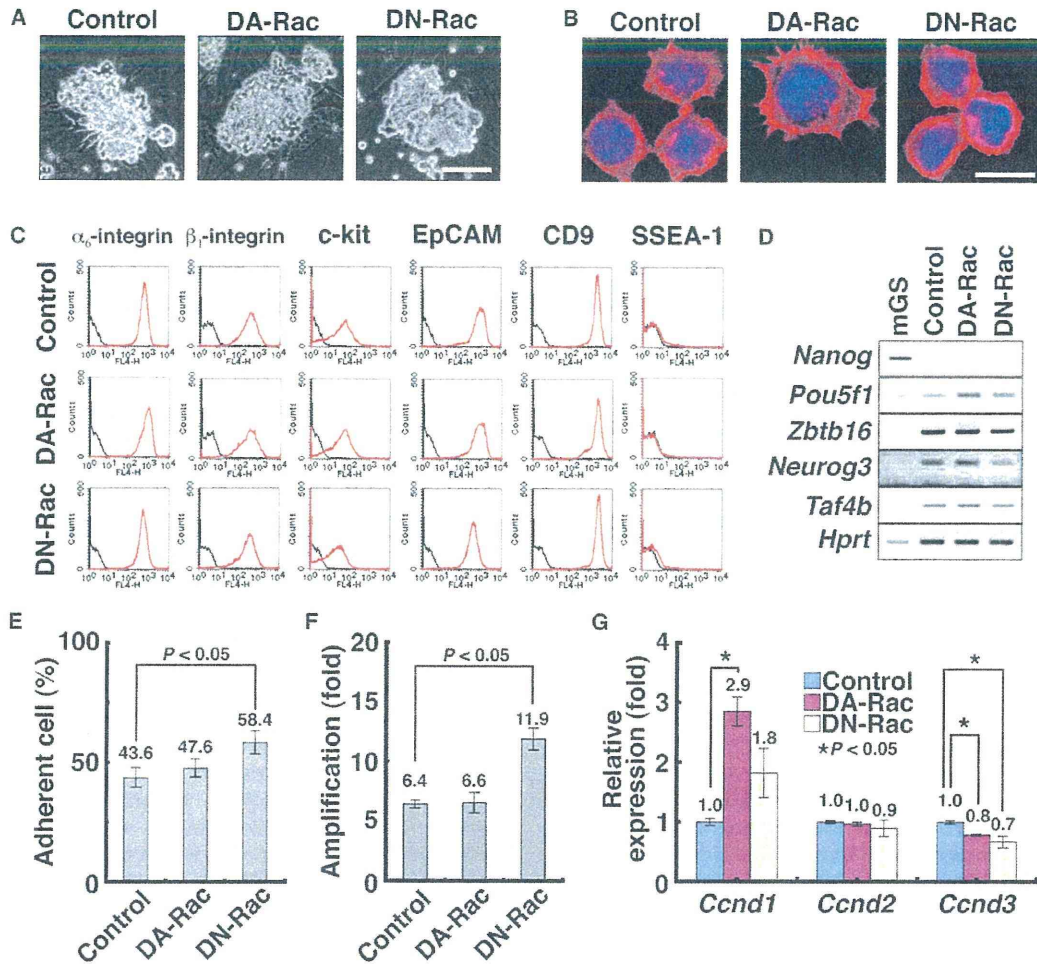


Figure 3. Characterization of DA-Rac and DN-Rac Cells

(A) Colony morphology on MEFs. (B) Microscopic appearance of transfectants. Cells were plated on laminin for 6 hr and stained with rhodamine-labeled phalloidin. Counterstain is with Hoechst 33342. (C) Flow cytometric analyses of surface molecules. Black lines indicate control staining. (D) RT-PCR analyses showing normal spermatogonia marker expression. mGS, multipotent GSCs (Kanatsu-Shinohara et al., 2004). These cells are rare occurrences in GSC cultures and express *Nanog*, unlike GSCs that are unipotent. (E) Enhanced laminin binding of DN-Rac cells. Cells were plated on laminin-coated plates for 30 min, and adherent cells were recovered by trypsinization. (F) Enhanced proliferation of DN-Rac cells. Cells were cultured on MEFs for 6 days. (G) Real-time PCR analyses of cyclin D expression levels (n = 6). Scale bar = 100 μ m (A); 10 μ m (B). Error bars = SEM. See also Figure S2 and Tables S1, S2, and S3.

increases in DN-Rac cells. Assuming that each colony is produced by one SSC and that seeding efficiency is 10% (Nagano et al., 1999), the doubling times of the SSCs during the 2 month period were 12.7, 13.2, and 15.7 days for the control, DA-Rac, and DN-Rac SSCs, respectively. We examined the expression of p27 cyclin-dependent kinase inhibitor (CDKI), because p27 KO SSCs also preferentially undergo differentiating divisions (Kanatsu-Shinohara et al., 2010). We found that p27 is significantly suppressed in DN-Rac cells (Figure 4E). These results suggest that the inhibition of Rac induced more differentiating divisions of SSCs in vivo during regeneration.

Transplantation into Immature Testis Rescues Defective Colonization of Rac1 KO SSCs

To understand the mechanism of the homing defect, we followed the pattern of donor cell colonization at different time points after transplantation (Figure 5A). Although LacZ-expressing cells were similarly found until 10 days posttransplantation, we were unable to find patches or networks of spermatogonia on the basement membrane, which occurs 2–3 weeks after transplantation. Considering the relatively slow doubling time of the SSCs after transplantation (~7.9 days) (Nagano, 2003), this observation suggested that the loss of the typical colonization pattern was

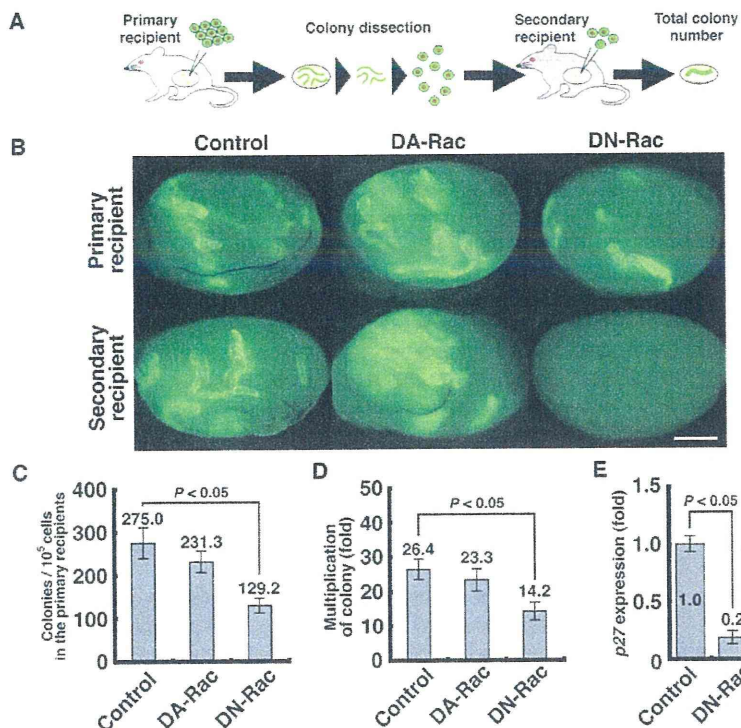


Figure 4. Serial Transplantation of GSCs

(A) Experimental procedure. GSCs were transplanted into W recipients (primary recipients). Two months after transplantation, EGFP-expressing germ cell colonies were dissected out using fine forceps, and enzymatically dissociated into single-cell suspensions. Portions of the cells were then transplanted into two testes of a W recipient (secondary recipients).

(B) Macroscopic appearance of recipient testes. Green fluorescence indicates donor cell colonization. Note the reduction of colonies in the recipients that received DN-Rac cells.

(C) Numbers of colonies in the primary recipients (n = 9 for the control; n = 12 for DA-Rac and DN-Rac cells).

(D) Multiplication of colony numbers (total regenerated colony number $\times 10^6$ / primary colony number used for serial transplantation) (n = 9 for the control; n = 12 for DA-Rac and DN-Rac cells).

(E) Real-time PCR analyses showing p27 downregulation in DN-Rac cells (n = 6).

Scale bar = 1 mm (B). Error bars = SEM. See also Tables S1 and S4.

not due to defects in proliferation and that the homing defect occurs at an early stage of colonization. SSC homing is thought to occur in several steps: attachment to Sertoli cells, passage through the tight junctions between Sertoli cells, and migration to the germline niche on the basement membrane (Nagano et al., 1999). To determine whether decreased SSC homing was caused by the defective migration of SSCs through the tight junctions between Sertoli cells, we next used immature 5- to 10-day-old recipient testes lacking tight junctions. The BTB develops around 12–14 days after birth, and immature pup testes before this period lack tight junctions between Sertoli cells and exhibit enhanced colonization of donor SSCs after transplantation (Shinohara et al., 2001). Although adult W mice were reported to have leaky BTBs in a previous study (Morrow et al., 2009), injection of dextran (~10 kD) or biotin (557 D) into the interstitium of pup, but not adult, W testes resulted in leakage into the adluminal compartment of the seminiferous tubules (Figure S3), showing the normal integrity of BTB in adult W mice.

Three experiments were performed, and approximately 1.2×10^5 *Rac1* KO or control cells were transplanted into pup testes after overnight incubation with AxCANCre in vitro. Cre treatment successfully deleted $68.6\% \pm 3.1\%$ (n = 3) of the floxed alleles, and analyses at 3 months after transplantation revealed significant colonization by SSCs lacking the *Rac1* gene (Figures 5B and 5C). Although testicular size was slightly smaller in recipients that received mutant cells, the difference was not significant (Figure 5D, top). Histological analyses showed comparable levels of colonization by mutant and control cells (Figure 5D, bottom). In total, $61.4\% \pm 7.9\%$ and $47.1\% \pm 4.2\%$ (n = 11) tubules showed spermatogenesis with control and mutant cells, respectively.

Both histological analyses and RT-PCR analyses confirmed normal differentiation of *Rac1* mutant cells (Figures 5B and 5E). Similar results were obtained using DN-Rac GSCs that showed reduced colonization (Figure 5F). We microinjected approximately 0.5 to 1.0×10^2 control and DN-Rac GSCs into pup seminiferous tubules, and the number of colonies was determined after 5 weeks. Compared with the adult recipients, the colonization efficiency of control and DN-Rac GSCs increased by 6.1- and 7.7-fold in the pup recipients, respectively. However, the difference between the two types of cells was not significant (Figure 5G). We then used the primary recipient testes for serial transplantation (Table S5). The number of cells recovered from the recipients ranged from 0.7 to 1.8×10^6 cells (average of 1.2×10^6 cells). In contrast to the adult recipient transplantation, the analyses of the secondary pup recipients revealed that DN-Rac GSCs produced significantly more colonies than did control cells (Figure 5H). Assuming that seeding efficiency is 100% in pup testes, the doubling times of the SSCs during the 5 week period were 7.8 and 6.1 days for the control and DN-Rac SSCs, respectively. Taken together, these results showed that loss of SSC activity in *Rac1* KO cells or DN-Rac cells was caused by the defective transmigration through the BTB.

Decreased Expression of Tight Junction-Associated Proteins in Rac Mutant Cells

The results described in the previous subsection suggested that *Rac1* KO SSCs have difficulty in migrating through the BTB. Because successful migration through the BTB would depend on the modulation of tight junction-associated protein expression on both SSCs and Sertoli cells, we hypothesized that homing defects were caused by abnormal expression of tight junction-associated adhesion molecules in SSCs. Therefore, we next examined the expression of occludin and claudins, components of tight junctions, in GSCs and W testis. RT-PCR